Kinematic Analysis and Optimization of Robotic Milling

by

Ömer Faruk SAPMAZ

Submitted to the Graduate School of Engineering and Natural Sciences

In partial fulfillment of

the requirements for the degree of

Master of Engineering

Sabancı University July 2019

KINEMATIC ANALYSIS AND OPTIMIZATION OF ROBOTIC MILLING

APPROVED BY:

Asst. Prof. Dr. Lütfi Taner Tunç
(Thesis Supervisor) .....

Prof. Dr. Erhan Budak .....

Asst. Prof. Dr. Umut Karagüzel .....

DATE OF APPROVAL: 12/07/2019

Dedicated to my beloved family...

ABSTRACT

KINEMATIC ANALYSIS AND OPTIMIZATION OF ROBOTIC MILLING

Ömer Faruk Sapmaz

Manufacturing Engineering MSc. Thesis July 2019

Supervisor: Lütfi Taner Tunç

Keywords: Tool axis optimization, Workpiece positioning, Robotic milling, 5-Axis machining

Robotic milling is proposed to be one of the alternatives to respond the demand for flexible and cost-effective manufacturing systems. Serial arm robots offering 6 degrees of freedom (DOF) motion capability which are utilized for robotic 5-axis milling purposes, exhibits several issues such as low accuracy, low structural rigidity and kinematic singularities etc. In 5-axis milling, the tool axis selection and workpiece positioning are still a challenge, where only geometrical issues are considered at the computer-aided-manufacturing (CAM) packages. The inverse kinematic solution of the robot i.e. positions and motion of the axes, strictly depends on the workpiece location with respect to the robot base. Therefore, workpiece placement is crucial for improved robotic milling applications. In this thesis, an approach is proposed to select the tool axis for robotic milling along an already generated 5-axis milling tool path, where the robot kinematics are considered to eliminate or decrease excessive axis rotations. The proposed approach is demonstrated through simulations and benefits are discussed. Also, the effect of workpiece positioning in robotic milling is investigated considering the robot kinematics. The investigation criterion is selected as the movement of the robot axes. It is aimed to minimize the total movement of either all axes or selected the axis responsible of the most accuracy errors. Kinematic simulations are performed on a representative milling tool path and results are discussed.

ÖZET

Robotik frezeleme endüstrinin esnek ve uygun maliyetli üretim sistemleri talebine cevap verebilecek bir alternatif olarak önerilmektedir. Robotik 5eksenli frezeleme operasyonları için kullanılmakta olan seri kollu 6 serbestlik dereceli robotlar düşük hassasiyet, düşük yapısal sertlik ve kinematik tekillikler vb. gibi çeşitli problemlere maruz kalmaktadır. 5 eksen frezeleme operasyonlarında kesici takım ekseni seçimi ve iş parçası konumlandırılması halen bilgisayar destekli imalat programlarında sadece geometrik açıdan değerlendirilen zorlu bir durumdur. Robotun ters kinematik çözümü örneğin eksenlerin pozisyonları ve hareketleri, robotun kaidesine göre iş parçasının konumuna bağlıdır. Bu nedenle, iyileştirilmiş bir robotik frezeleme operasyonu için iş parçası konumu seçimi çok önemlidir. Bu tezde, önceden oluşturulmuş bir 5-eksen takım yolu boyunca kesici takım ekseni seçimi için bir yaklaşım önerilmiştir, burada robot kinematiği göz önünde bulundurularak aşırı eksenel dönüşler ortadan kaldırılmaya yada azaltılmaya çalışılmıştır. Önerilen yaklaşım simulasyonlarla gösterilmiş ve faydaları tartışılmıştır. Ayrıca, iş parçası konumlandırmanın robotik frezelemedeki etkisi robot kinematiği göz önüne alınarak araştırılmıştır. Robot eksenlerinin hareketi inceleme kriteri olarak seçilmiştir. Tüm eksenlerin toplam hareketini en aza indirmeyi veya hataların çoğundan sorumlu en hassas eksenlerin kullanımını en aza indirmek amaçlanmıştır. Kinematik simulasyonlar temsili bir takım yolu üzerinde yapılmış ve sonuçlar tartışılmıştır.

ACKNOWLEDGEMENTS

In the first place, I would like to express my deepest appreciation to my thesis advisor, Assistant Prof. Dr. Lütfi Taner Tunç, for his patience, motivation, enthusiasm, and immense knowledge. I could not have imagined having a better advisor and mentor for my master study.

I would like to express my sincere gratitude to my committee member Professor Dr. Erhan Budak, for his emotional and motivational support, his precious comments and guiding attitude. As my teacher and mentor, he has taught me more than I could ever give him credit for here. He has shown me, by his example, what a good scientist (and person) should be.

I would like to thank my committee member, Assistant Prof. Dr. Umut Karagüzel for his encouragements and valuable comments.

I would like to extend my sincere thanks to my colleagues and the robotic manufacturing team of KTMM for their support and time. Special thanks to my dear friends Bora, Canset, Başak, Fatih, Esra for all the enjoyable times we shared together.

Finally, I must express my very profound gratitude to my parents Seher and Tuna for continuous encouragement throughout my life and the process of writing this thesis. This accomplishment would not have been possible without them. Thank you.

TABLE OF CONTENTS

LIST OF FIGURES

LIST OF TABLES

LIST OF SYMBOLS AND ABBREVITIONS

CNC	Computer Numerical Control
NC	Numerical Control
DOF	Degree of Fredom
CAM	Computer Aided Manufacturing
CL	Cutter Location
CC	Cutter Contact
TA	Tool Axis
D-H	Denavit-Hartenberg
WCP	Wrist Center Point
WCS	World Coordinate System
F	Feed
N	Surface Normal
C	Cross feed
FCN	Feed-Croos Feed- Normal Coordinate System
S.n	Sub-node
θ_i	Joint Angle is D-H parameter
a_i	Link Length is D-H parameter
d_i	Link Offset is D-H parameter
α_i	Link Twist is D-H parameter
β	Roll angle

α	Pitch Angle
γ	Yaw angle
R_e^0	End effector orientation and position matrice wrt base
R_e^c	End effector orientation and position wrt wrist center

1 INTRODUCTION

1.1 Background of the study

Robotics is a contemporary field which crosses with conventional engineering disciplines therefore robotics and applications require expertise of mechanical engineering, electrical engineering, system and industrial engineering, computer science and mathematics. The robot term, first introduced to vocabulary by Czech playwright in 1920 and the word Robota means working, in Czech. From then the term has been covered a great variety of mechanical devices such as industrial manipulators, autonomous mobile robot and humanoids [1]. The robot term is defined officially as re-programmable and versatile manipulator designed to move material and parts, or specially designed mechanisms through variable programmed motions for the utilization of variety of tasks [2].

Recent progresses in machining and tool design technology, most particularly milling operations indicates the necessity for flexibility to respond the diversity of the manufacturing market, reduction in the weight and dimensions, high quality, accuracy and global economic trends [3]. This progress resulted to development of machine tools of high precision and accuracy however manufacturing engineering objectives still evolving, and the requirements shows that industry focal points as high volume and flexible manufacturing to compete in terms of economy. Flexibility concerns to use same facility minor-major changes therefore an industrial robot can fulfill the demands current and future of manufacturing industry in a cost-efficient manner. The use of robots for material handling and welding processes achieved outstanding results in manufacturing and production industry. After successful utilization of robots for such purposes the machining purposes robots have emerged. Robotic machining, as a tool positioning system with the help of flexible kinematics of the industrial

manipulators are capable of machining parts complex detail and shapes, that conventional machine tools (CNC) needs special fixtures and techniques to produce. Further robotic machine tools are capable to machining large parts in single setup with the help of large working envelope such as 7.5 m^3 and with rotation it can cover up to 20m^3 [3]. Robots have advantages such as mobility and reconfigurability however use of robots for machining purposes involves several issues related to accuracy, static and dynamic stiffness and robustness. Considerable amount of research has been done to improve accuracy and dynamic stiffness of robots for machining applications. The fundamental research includes kinematic, control, programming and process improvement. Robots can be classified with respect to main criteria such as degree of freedom, structure, drive system and control. One major classification is to categorize robots with respect to degrees of freedom. In most cases, industrial robots contain 6 degrees of freedom (DOF) to manipulate an object in the space by translations and rotations. Another category is defined by the structure of the robot, which is open-loop serial chain and closed loop parallel chain (see Figure 1-1). In the former, the topology of the robot takes the kinematic structure form of an open-loop chain. In the latter, the topology of the robot is formed as closed loop chain called, the combination may be named as the hybrid manipulators.

(a) Serial robot (b) Parallel robot

Figure 1-1: Robot Types

Generally, robot manipulators are electrically, hydraulically or pneumatically driven. Most of the robots use direct current or alternative current servo motors or stepper motors by the reason of clean, cheap, quiet and relatively easy control. Hydraulic drives mostly used to lift the heavy loads. The drawbacks of hydraulic drives are maintenance and noise and control issues. The workspace of the robot is defined as reaching capability of the end-effector (see Figure 1-2), a reachable workspace which is suitable to reach by at least one orientation. The dexterous workspace is defined as the end-effector reachable space by more that all possible orientations.

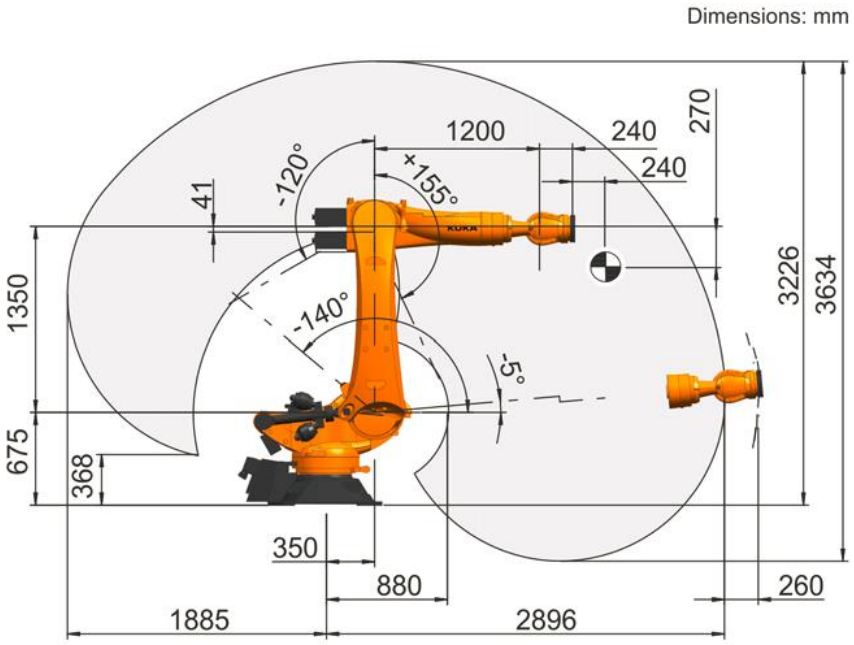

Figure 1-2: Kuka kr240 r2900 dimensions and workspace [[4]]

The accuracy of the robot is measured by commanding the robot to move at point in workspace and repeatability is the difference between results of the successive motion [[5]].

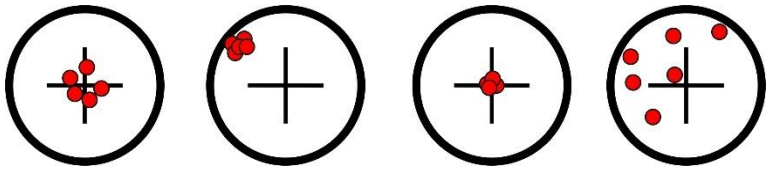

(a) (b) (c) (d)

Figure 1-3: a) Accurate, b) Repeatable, c) Accurate and repeatable, d) Not accurate and repeatable

In Figure 1-3, the commanded point is the center of the circle, the distributions of the points indicate the accuracy and repeatability capabilities of the industrial manipulator. The positioning errors mostly dealt with position encoders located at the motors or joints. Accuracy is mostly affected by flexibility such as bending of the links under gravitational loads, gear backlash static and dynamic effects [6]. Repeatability of the robots mostly related with controller resolution the minimum motion that the controller that able to sense it is also dependent on the encoder accuracy [5].

Robots have different characteristics than the conventional machine tools the comparison on the other hand the robot characteristic vary between serial manipulator and the parallel manipulator which is shown in Table 1-1 [5].

Feature	Serial Manipulator	Parallel Manipulator
Workspace	Large	Relatively Small
Forwards kinematic analysis	Relatively Easy	Difficult
Inverse kinematic analysis	Relatively Difficult	Simple
Stiffness	Low	High
Inertia	Large	Small
Payload/weight	Low	High
Speed and acceleration	Low	High
Accuracy	Low	High
Calibration	Low	High
Workspace/footprint	High	Low
Number of applications	High	Low

Table 1-1: Characteristics of the serial arm and parallel robots

And the comparison between conventional CNC and robots in terms of different parameters shown in Table 1-2 [7].

Parameter	CNC machine	Industrial robot
Accuracy	0.005 mm	0.1-1.0 mm
Repeatability	0.002	0.03-0.3
Workspace	Low	Large
Complex Trajectory	Suitable for 3-5 axis machining	Any complex trajectory
Stiffness	High	Low
Dynamic properties	Homogenous	Heterogenous
Manufacturing flexibility	Single or similar	Any type
Price	Relatively high	Relatively low

Table 1-2: CNC and serial arm robot comparison

1.2 Research Objectives

The objective of this thesis is to meet need of the optimization of robotic milling processes by selection of the optimal tool axis considering robot kinematics for a continuous 5-axis tool path and selection of the feasible workpiece location by considering kinematics of the industrial robot.

In order to achieve this objective, the necessary steps are taken as follows,

1) Acquire the surface data from CAM software
2) Calculate the rotational angles for each drive of the robot
3) Determine the feasible tool axis region on the tool path
4) Create all the possible tool axis position for all CL-points
5) Employ the Dijkstra's shortest path algorithm
6) Select optimum continuous tool axis for every CL-point
7) Discretize the worktable in regions
8) Calculate the tool path for each region
9) Determine feasible region for positioning

1.3 Organization of thesis

The thesis is organized as follows: In Chapter 1, literature review is given in relation to the objectives of the thesis. This is followed by the kinematic analysis of 6-axis industrial robots in Chapter 2, where Denavit-Hartenberg [8] approach in kinematic analysis and the required parameters for KUKA KR240 R2900 robot are explained. Afterwards, an alternative solution method [9], which relies on decoupling of the robot kinematics, is discussed. Chapter 2 is concluded by providing a comparison of these two methods are compared in terms of simplicity and general application. Chapter 3 presents explains the geometry of 5-axis milling, which is followed by the effects of tool axis on robotic 5-axis milling. Chapter 3 is continued by presenting the tool axis optimization approach for a robot to perform a continuous 5-axis milling cycle. Workpiece location selection based on kinematics is introduced in Chapter 4. Finally, the conclusion and contributions are presented with the future potential of the research.

1.4 Literature Review

Robot manipulators were first designed to perform tasks such as pick-place and material handling [10] back in 1960s. After their successful utilization in material tending, the use of assembly took place. This if followed by tasks involving trajectories such as spray painting [11], welding [12] and machine tool tending [13]. Nonetheless, utilization of industrial robots for material removal processes, i.e. machining, came to consideration back in 2000s [14], which became a trending application for the last decades especially for the large-scale parts in the aerospace, naval and nuclear industries. Yet, 80% of industrial robots are solely assigned to relatively non-complex operations such as material handling and welding etc. and less than %5 of the robots used for material removing operations [15].

In multi axis milling operations, the additional rotational degrees of freedom to orient the tool axis, do not only complicates the dynamics and mechanics of the process through cutting coefficients and stability but also the motion of the machine tool may become complicated

due to excessive rotations to satisfy the tool orientation at any cutter location (CL) point along the tool path [16]. In computer aided manufacturing (CAM) applications, calculation of the tool axis is driven by workpiece geometry and smoothness issues [17]. In the literature the effects of the lead and tilt angles on process and the machine tool kinematics have been studied by several researchers. In the study of Ozturk et. al [18] the lead and tilt angle effects investigated through 5-axis ball end milling processes. This research showed that the tool orientation significantly affects the cutting forces and form errors due to tool deflection and eventually the proper tilt configuration can increase stability limit up to 4 times. However, in this study the kinematics of the machine tool axis and actual machining time was not considered. Later, Tunc [19] et. al addressed the machining time and machine tool motion. The method introduced by Makhanov et. al [20] analyzed the optimal sequencing of the rotation angels for five axis machining and developed an algorithm for reduced kinematical errors based on shortest path optimization. The cost function is defined as the angle variation for the shortest path algorithm. The minimization of the total angle variation for rough cuts leads to a significant accuracy increase up to 80%. Similarly, Munlin et al. [21] studied on optimization of the rotary axis around stationary points in 5 axis machine tools. They used shortest path algorithm and improved the accuracy of the machine tool motion by 65% in rough cutting operations.

To adapt industrial robots for machining operations and to benefit from their flexibility. Research efforts in robotic machining applications, gained momentum for the last two decades [14], [22]. In one of the very early studies by Matsuoka et al. [14] done in 1999. The behavior of the robot was investigated in a typical milling operation. The study showed that the increased spindle speed has a drastic effect on the cutting forces, by increasing the 80% of the spindle speed the cutting forces decreased to 50-70%. It was also identified that low frequency vibration modes around 25 Hz at high amplitudes, were introduced by the industrial robot, which is usually not the case in CNC machining applications. After the first application of industrial robots in machining processes, the researchers focused on implementing modelling approaches to identify improved machining conditions. It is noteworthy to state that, usually the stiffness values of joints and inertial parameters of links are not provided by the robot manufacturers. Therefore, identification of stiffness matrix requires an intense testing effort [25]. Abele et al. [22] modelled robot stiffness matrix to

determine the robot's deflection under machining conditions. In two other studies, Dumas et al. [23] and Abele et al. [24] proposed an approach to identify the joint stiffness of industrial robots to predict their response to cutting forces, with the aim of improving robotic milling processes. In another study, Zaeh et al. [26] offered a model based fuzzy algorithm to change control strategy of the robot in different stages of machining process to eliminate the static path deviation by considering the robot stiffness. Later, Schneider et. al [27] analyzed the error sources of the during machining identified the most effective two source as compliance and backlash. Demonstrated the robot posture dependency with position and frequency analysis then identified the stiffest posture of the robot.

Machining dynamics in robotic milling has been another important topic for investigation. In one of the very first studies, Pan et al. [28] stressed the differences between CNCs and industrial robots in terms of response to dynamic machining forces, where they claimed that the dominant source of vibration is mode coupling chatter due the high compliance of the structure and proposed suitable parameters for robotic milling through experimental results. Later, Zaghbani et. al [29] utilized the spindle speed variation approach to avoid chatter vibrations for improved chatter stability. Tunc and Shaw [30], investigated robotic milling in terms of the position dependent dynamics, feed direction effect on tool tip dynamics. In most of the stability analysis in CNC machining, the effect of cross transfer functions (CTF) is ignored. However, Tunc and Shaw [30], identified that the cross-transfer function (CTF) arising due to kinematic chain of the robot may significantly affect stability limits. Then, Tunc and Stoddart [31] experimentally determined the effects of the position dependency and cross transfer functions on stability and propose a proper setup for tooling and variable spindle speed to increase productivity.

In multi axis machining, the workpiece is attached to the work table randomly, in most of the cases. However, workpiece placement with respect to the machine tool base is a critical decision, especially in 5 axis milling operations, which may affect the rotary axis motions and actual feed rate, actual cycle time and part quality [32], [36]. In this direction, i.e. identification of the appropriate workpiece locations, considerable amount of research has been conducted in literature. Pessoles et al. [32] proposed a method for continuous 5 axis

milling operations and they applied it on a five-axis tilt rotary table CNC machine tool. The aim of their study is to minimize the overall distance travelled by the machine tool axis. They used the forward and inverse kinematic solution of the machine tool kinematic chain. This work proved that careful selection of the workpiece location can significantly reduce the actual machining time on the machine tool. The main goal is to eliminate unproductive motion of the rotary axis. The experimental part of the study showed that when the workpiece location is selected based on machine tool motion, the actual machining time can be decreased by 24% also with combination with greater reachable feed rate the timesaving can be increase up to 40 percent with respect to an arbitrarily selected workpiece location. Later, Yang et al. [33] proposed a method for selection of the workpiece placement by considering the tracking errors for 5-axis machining applications. In their study, the workpiece placed on a worktable to minimize the transmitted torque to the rotary and the translation axis of the machining unit. The method is applied on a 5-axis machining unit with a tilt worktable. The cutting forces that transmitted to the axes of the table identified by kinematic modelling of the machining unit. Then separating the table into regions and by solving the inverse kinematics, the preferable regions were identified. The proposed optimization algorithm is experimentally validated on a 5-axis machine tool. As a result of this study the transmitted cutting torque to the rotary drives decreased significantly. Thereby, the tracking errors reduced as well so that the disturbance load on the rotary axis reduced, leading to 68% increase in the contouring accuracy. In another research, Anotaipaiboon et al. [34] investigated the optimal setup in 5-axis milling and presented an optimization approach for minimized kinematic errors that raised from the initial configuration composed of the position and the orientation of the workpiece on the worktable. In their study, for a given tool path the optimal workpiece location determined by the least square's method. The main constraints used as the scallop height, local and global accessibility. The algorithm is experimentally validated, and the results showed that the machining accuracy increased substantially. Next, the study of Lin et. al [35] proposed a method to eliminate the non-linear errors due to the nonlinear motions of the rotary axis of a table tilting machine tool. According to nonlinear evaluation of the method with rotational tool center point considered as a workpiece setup function afterwards the particle swarm optimization method the optimal

location is determined. The proposed algorithm was tested, and the results showed that the z direction does not significantly affect the nonlinear errors.

Workpiece location selection is an important topic for robotic machining processes to reach better surface quality and machining tolerances in robotic milling. In study of the Dumas et. al [36] workpiece placement in robotic milling was investigated, where elasto-static stiffness model of the robot was developed and used for workpiece positioning. As case study, they used KUKA KR270-2 industrial robot. The cutting forces that acts on the robot was also considered and with help of the 6^{th} axis of the robot the additional redundancy is investigated. The researchers performed a hybrid optimization approach and compared the machining quality in four case studies. Namely, optimum workpiece positioning with the best and worst redundancy planning, worst workpiece positioning with best and worst redundancy. The results of this study indicated that positioning of the workpiece can increase machining quality by 14 times compared to the worst case of random placement. In another study, Lopes et al. [37] investigated workpiece selection by considering the power consumption of the robot by applying a single objective genetic algorithm. They found out that there is more than one feasible solution for parallel hexapod robots. In this study, the stiffness of the manipulator and dynamic model were also considered, and the feasible workpiece location selected with the help of multi-objective genetic algorithm. However, the researchers didn't include issues such as machining forces acting on the robot and the effect of robot trajectory. Later, Lin et al [38] introduced a posture optimization methodology for 6 axis industrial manipulators and evaluate the machining performance. They identified that the deformation map by considering the forces acting on the end effector of the robot and related main body stiffness index also identified. Overall performance map is determined to optimize robot posture and eventually the workpiece positioning was done regarding the optimized robot posture. However, in this study they only considered kinematic and static performance, so that the dynamic performance is the main absence in this study to select best machining posture especially for workpiece positioning for machining operations. In another research, Vosniakos and Matsas [39] showed the feasibility of the robotic milling through the robot placement. They implemented two different genetic algorithms to deal with robot kinematics for the purpose of maximum manipulability and to minimized joint torques for a milling application. In their study, the first algorithm explored the optimum initial position of the end

effector that enables the maximum kinematic and dynamic manipulability in milling. The second algorithm investigated the initial positioning of the end effector to minimize the torques in the first three joints while performing whole cutting operation. The second algorithm considered the cutting forces that influence the torques required by the joints. This study contributed to the use of robots for heavy torque operations and on the other hand by minimizing the torques for a cutting operation enables the smaller robots to be implemented for such purposes.

1.5 Summary

These studies indicate that the optimization of the posture and the workpiece location for robot provides significant improvements on the machining performance. Contrary to listed literature above posture optimization for robotic 5-axis milling processes such that tool orientation and workpiece location still needs further investigation. Most of the research investigated the adaptation of the robot for machining in terms of stiffness characteristics and aimed error compensation however not all robotic machining application exposed to high cutting forces such that grinding and polishing. On the other hand, these are time consuming and costly operations so that should be utilized in optimal conditions in terms of kinematics. Therefore, the minimization of the axes usage is a critical topic that may lead accuracy improvement.

2 ROBOT KINEMATICS

Kinematics is the analytical study of the motion of mechanical points, bodies and mechanism. Kinematics does not consider physical and dynamical entities namely, force torque etc. Mainly refers geometry of the motion by modelling it using mathematical expressions and algebra. Mechanic of the robot manipulator mostly represented by kinematic chains of the rigid bodies connected as shown in (Figure 2-1). Formulation of the robot kinematics is required to analyze the robot movement for any purpose. The robot kinematic analysis is separated into two main problems; namely forward and inverse kinematics. The forward kinematics essentially deals with derivation from the joint space to cartesian space coordinates. As the name implies, inverse kinematics deals with identification of the joint set when the required position of the robot in cartesian space, is known. Forward kinematics is relatively simple to solve than the inverse kinematics as inverse kinematics may require the highly non-linear equations to be solved and the kinematic redundancy to dealt with singularity issues.

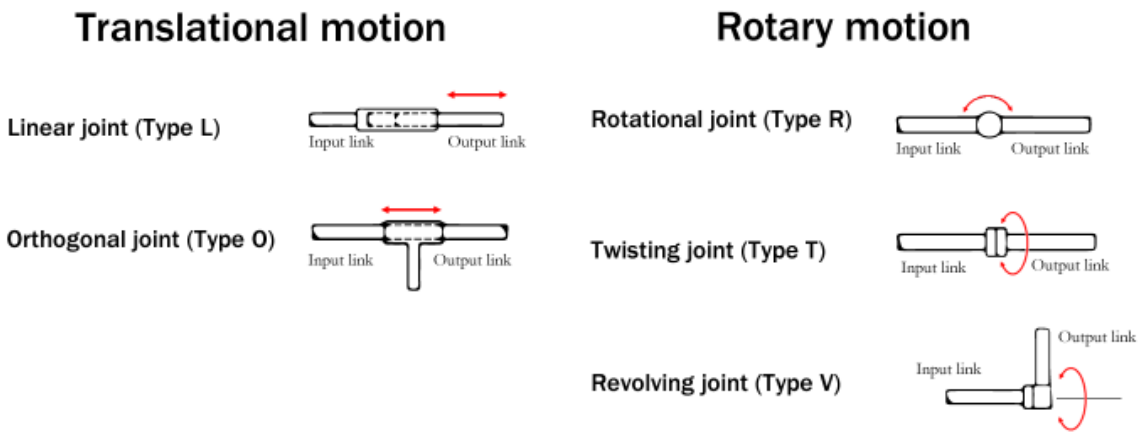

Figure 2-1: Joint Types

The first arm connected to the base of the manipulator and the end effector is the end of the chain. The resulting the motion is obtained by composition of transformation matrices with respect motions of the attached link to each other.

2.1 Denavit-Hartenberg Method

In this section the Denavit-Hartenberg [8] method also well known as D-H is explained in detail. The forward kinematics, defined as the relation between the individual joints that connects rigid body's (arms) of the robot manipulator and the last arm namely end effector of the robot. Or in other words, to determine of the end effector position and orientation in terms of the joint variables such as angle for a rotational joints and link distance for prismatic joints of the robot. In this convention each homogenous transformation A_i contains four simple transformations:

$$A_i = Rot_{z,\theta_i} Trans_{z,d_i} Trans_{x,a_i} Rot_{x,\alpha_i} \tag{2.1}$$

$$= \begin{bmatrix} c_{\theta_i} & -s_{\theta_i} & 0 & 0 \\ s_{\theta_i} & c_{\theta_i} & 0 & 0 \\ 0 & 0 & 1 & 0 \\ 0 & 0 & 0 & 1 \end{bmatrix} \begin{bmatrix} 1 & 0 & 0 & 0 \\ 0 & 1 & 0 & 0 \\ 0 & 0 & 1 & d_i \\ 0 & 0 & 0 & 1 \end{bmatrix} \begin{bmatrix} 1 & 0 & 0 & \alpha_i \\ 0 & 1 & 0 & 0 \\ 0 & 0 & 1 & 0 \\ 0 & 0 & 0 & 1 \end{bmatrix} \begin{bmatrix} 1 & 0 & 0 & 0 \\ 0 & c_{\alpha_i} & -s_{\alpha_i} & 0 \\ 0 & s_{\alpha_i} & c_{\alpha_i} & 0 \\ 0 & 0 & 0 & 1 \end{bmatrix} \tag{2.2}$$

$$= \begin{bmatrix} c_{\theta_i} & -s_{\theta_i} c_{\alpha_i} & s_{\theta_i} s_{\alpha_i} & a_i c_{\theta_i} \\ s_{\theta_i} & c_{\theta_i} c_{\alpha_i} & -c_{\theta_i} s_{\alpha_i} & a_i s_{\theta_i} \\ 0 & s_{\alpha_i} & c_{\alpha_i} & d_i \\ 0 & 0 & 0 & 1 \end{bmatrix}$$

Where, the quantities $\theta_i, a_i, d_i, \alpha_i$ are the parameters related to link *i*, and joint *i.* They are named as joint angle, link length, link offset and link twist, respectively. Matrix A has a single variable so that the four parameters are constant and only θ_i is the joint variable. If the joint is prismatic, joint variable is d_i. (See Figure 2-1: Joint Types)

Representation of any arbitrary homogenous transformation matrix using only 4 variables is not possible. In D-H representation, frame *i* is rigidly attached to link *i* and by doing so, the

selection of frame *i* on link *i* in a practical manner can reduce number of the parameters which are necessary to represent a homogenous transformation matrix.

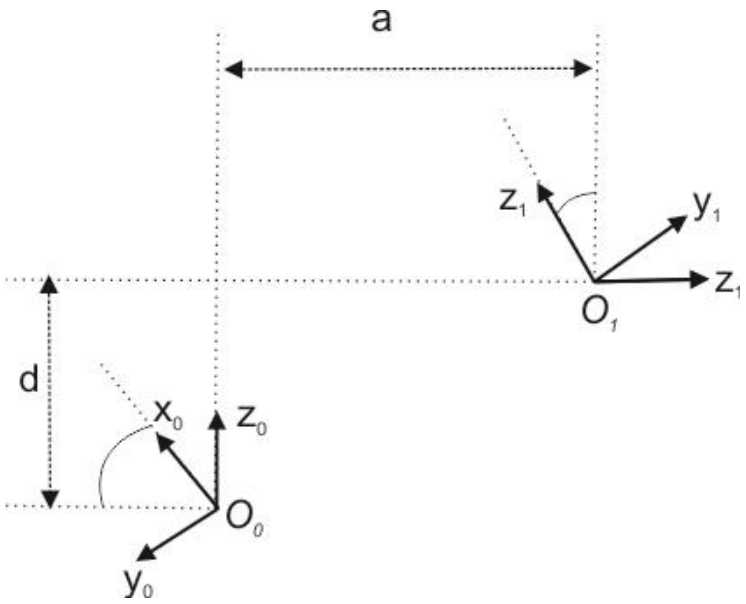

Figure 2-2: Homogenous transformation O_0 to O_1

In Figure 2-2, given 2 coordinate frames in the space O_0, O_1 which has a homogenous transformation matrix that takes the coordinates of the frame 0 to frame 1. So that the homogenous transformation matrix that changes the coordinates of the frame 1 to 0.

D-H Frame Assigning Rules

An arbitrary homogenous transformation matrix is constructed by 6 parameters 3 parameters for positioning and 3 parameters for orientation such as Euler angle [40]. As stated earlier in D-H convention only 4 parameters are needed to build a transformation matrix by following the two rules of this convention.

Rule 1: The axis x_1 is perpendicular to the axis z_0.

Rule 2: The axis $x_1$intersects the axis z_0.

Figure 2-2, obeys D-H rules so that the transformation matrix can be built by using only four parameters, which are *a, d,* α and θ. The implemented D-H rules on a joint and link are shown in Figure 2-3 so that the physical meaning of these parameters is defined as below:

a : The parameter *a*, is the distance between axes z_0 and z_1. The distance measured along the x_1 axis.

α : The parameter α, is the angle between the axes z_0 and z_1. The angel measured in a normal plane to x_1 and the direction obeys the right-hand rule.

d : The parameter *d*, is the distance between from the origin O_0 to the intersection point of the x_1 axis and z_0. The distance measured along the z_0 axis.

θ : The parameter θ, is the angle between x_0 and x_1 measured in a plane to z_0

2.1.1 Assigning the coordinate frames

In order to assign frames of industrial robots D-H rules must be satisfied, and the frames should be starting from 0 to last frame *n*. To start with the assignment of Z_i axes, the axes Z_0 to Z_{n-1} are chosen arbitrarily. However, the Z axes must be along with the actuation axis. In Figure 2-3, it can be seen that Z_i is assigned to the axis of actuation of the $i+1^{th}$ link. So that, Z_0 is the actuation of joint 1 and Z_1 for joint Z_2 and so on for up to last joint. If the joint is revolute Z_i is the axis of revolution of joint i+1. After such assignment, the base frame needs to be specified intuitively. The only rule about the selection of the base frame is that it must lie on a point along Z_0 axis. Then, X_0 and Y_0 axes need to be selected freely taking into account the right-hand rule.

After frame 0 is constructed, the other frames are constructed in a sequential manner. Frame i, is defined by using frame i-1 and following D-H rules. There are special cases that must be taken account as explained in below;

1. The axes Z_{i-1} and Z_i are not coplanar, in this situation the unique line between the consecutive Z axes that has a minimum length. Theses line between Z_{i-1} and Z_i also defines the X_i. The origin O_i is defined by the point X_i intersects Z_i. The axis Y should

follow the right-handed frame rule. By applying this procedure, D-H rules are satisfied, and the transformation matrix is constructed.

2. The axes Z_{i-1} and Z_i coincides, in this case the axis X_i must be selected normal to plane of the Z_i and Z_{i-1}. The positive direction for the X_i is chosen arbitrarily. Selection of the O_i on the intersection point of the Z_i and Z_{i-1} the parameters a_i becomes 0.
3. The axes Z_{i-1} and Z_i are parallel, in this situation there are infinitely common normal between the axes so that first D-H rule cannot fully determine the X_i axis. So that the origin O_i can be selected on a point that lies on the Z_i axis. After selectin X_i axis the Y_i axis must follow the right-hand rule.

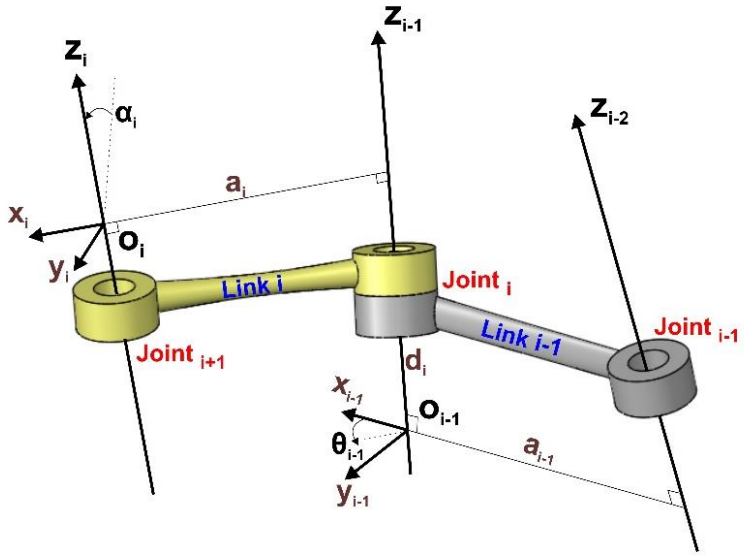

Figure 2-3: D-H frames and joints

These procedures are followed by frames 0 to n-1 for n-link robot. The last coordinate system $O_nX_nY_nZ_n$ is commonly called as end effector of the robot. The unit vectors along the end effector frame axes x, y, z is defined as n, s and a respectively. The axis terminology rooted directions of the gripper such as the approach direction called as letter *a*, the slide direction called as letter *s* and the normal direction called as letter *n*.

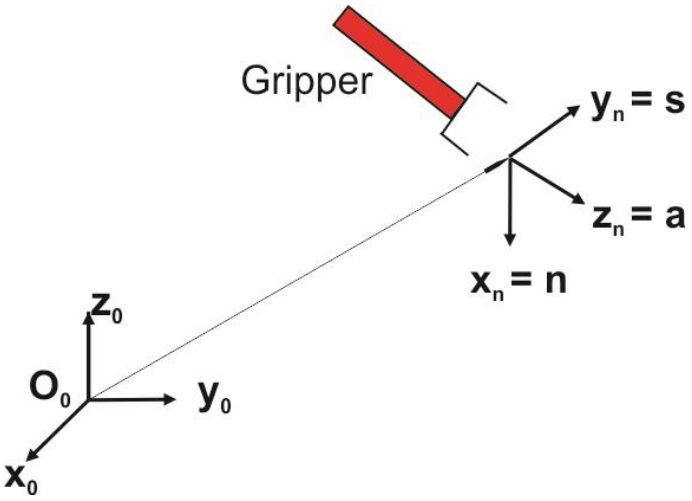

Figure 2-4: End effector frame

The example for simple two link robot arms, and the frames assigned according to Denavit-Hartenberg rules is given in Figure 2-5.

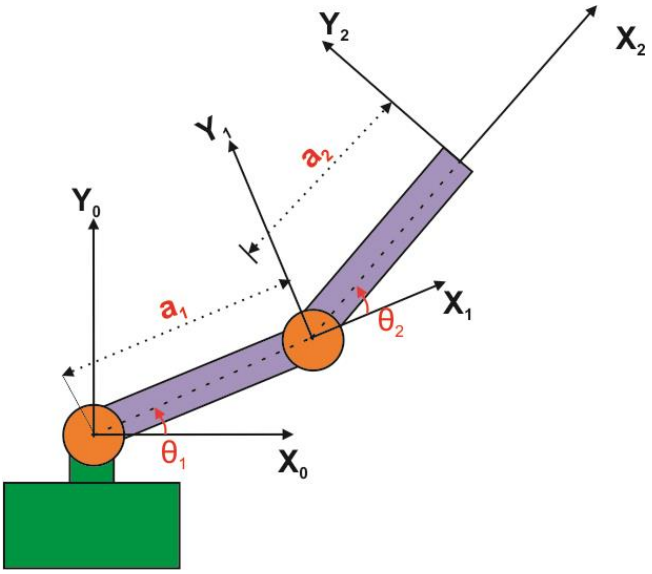

Figure 2-5: D-H convention for two arm planar robot

The Z_0 and the Z_1 axes have the direction in to page where the actuation points on the joints. The common origin of these frames is the intersection point of the Z and X axes and the Y

axes is specified according to right hand frame rule. D-H parameters of this case is shown below.

Link Number	a_i	α_i	d_i	θ_i
1	a_1	α_1	d_1	θ_1
2	a_2	α_2	d_2	θ_2

Table 2-1: D-H parameters for two arm planar robot

$$A1 = \begin{bmatrix} c_{\theta_1} & -s_{\theta_1} & 0 & a_1 c_{\theta_1} \\ s_{\theta_1} & c_{\theta_1} & 0 & a_1 s_{\theta_1} \\ 0 & 0 & 1 & 0 \\ 0 & 0 & 0 & 1 \end{bmatrix} A2 = \begin{bmatrix} c_{\theta_2} & -s_{\theta_2} & 0 & a_2 c_{\theta_2} \\ s_{\theta_2} & c_{\theta_2} & 0 & a_2 s_{\theta_2} \\ 0 & 0 & 1 & 0 \\ 0 & 0 & 0 & 1 \end{bmatrix} \quad (2.3)$$

The transformation matrix $T_1^0 = A_1$ so that the $T_2^0 = A_1 A_2$ and calculated as

$$T_2^0 = \begin{bmatrix} c_{\theta_1} c_{\theta_2} & -s_{\theta_1} s_{\theta_2} & 0 & a_1 c_{\theta_1} + a_2 c_{\theta_2} \\ s_{\theta_1} s_{\theta_2} & c_{\theta_1} c_{\theta_2} & 0 & a_1 s_{\theta_1} + a_2 s_{\theta_2} \\ 0 & 0 & 1 & 0 \\ 0 & 0 & 0 & 1 \end{bmatrix} \quad (2.4)$$

2.1.2 The implementation of the Denavit-Hartenberg method for KUKA KR240 R2900

In order to mathematically model a robot and gather the position and orientation of the end effector with respect to the other frames and base frame, D-H approach is used. The base frame is assigned as $X_0Y_0Z_0$ and other frames are assigned as shown in Figure 2-3 based on the discussion provided in the previous section the necessary steps and the rules are followed to build frames and directions. The Red Green Blue in Figure 2-6 corresponds to X, Y, Z

respectively. The resulting D-H parameters are given in Table 2-2. The manufacturer specs used as a reference to determine the positive directions for revolute joints and other D-H parameters (see Figure 2-7). Afterwards the homogeneous transformations between the frames taken in to account to calculate the end effector position coordinates with respect to base frame.

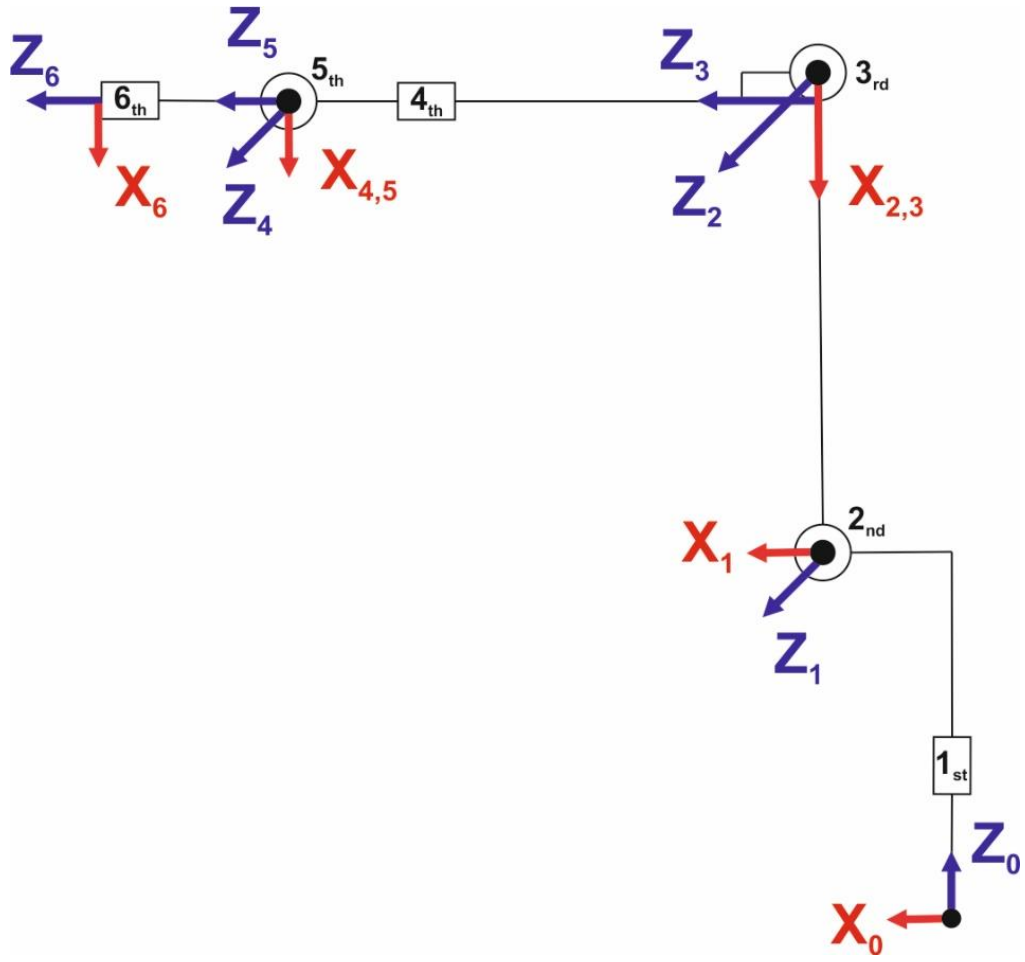

Figure 2-6: Kuka Kr240 R2900 DH frames

i	Theta (degree)	d (mm)	A (mm)	Alfa (degree)
1	θ_1	D_1= 675	A_1=350	α_1=-90
2	θ_{2+90}	D_2=0	A_2=1350	α_2=0
3	θ_3	D_3=0	A_3=41	α_3=90
4	θ_4	D_4=1200	A_4=0	α_4=-90
5	θ_5	D_5=0	A_5=0	α_5=90
6	θ_6	D_6=240	A_6=0	α_6=0

Table 2-2: D-H parameters for kuka kr240 r2900

The manufacturer specs for Kuka Kr240 r2900 are given in Figure 2-7. The positive direction of the joints and the dimensions of the robot are provided.

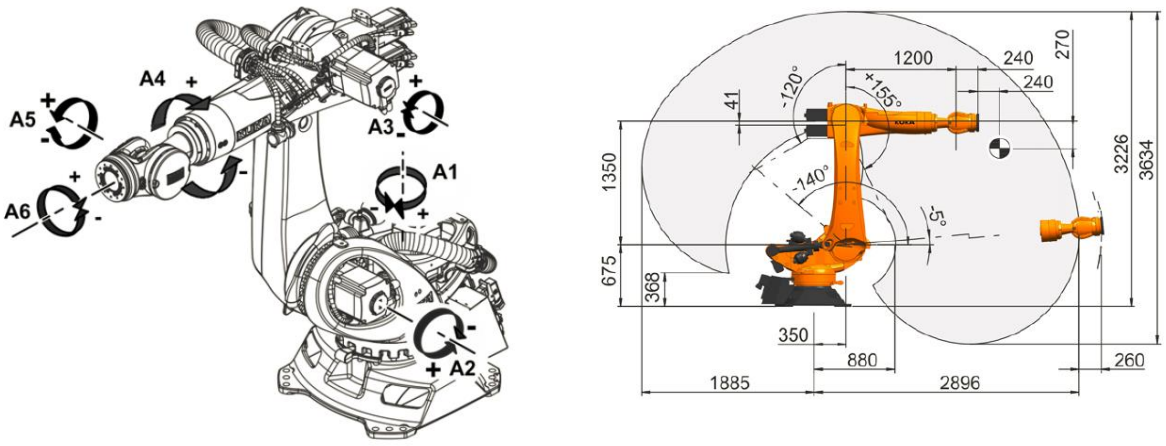

Figure 2-7: Datasheets of kuka kr240 r2900 [[4]]

The transformation matrices required to calculate the coordinates of each frame with respect to sequential frame are identified equation 2.5 to 2.10. In each transformation frame the related D-H parameters are utilized.

$$T_1^0 = \begin{bmatrix} cos_{\theta_1} & 0 & -sin_{\theta_1} & 0.350 * c_{\theta_i} \\ sin_{\theta_1} & 0 & cos_{\theta_1} & 0.350 * s_{\theta_i} \\ 0 & -1 & 0 & 0.675 \\ 0 & 0 & 0 & 1 \end{bmatrix} \tag{2.5}$$

$$T_2^1 = \begin{bmatrix} cos_{\theta_2} & -s_{\theta_2} & 0 & 1.350 * cos_{\theta_2} \\ sin_{\theta_2} & cos_{\theta_2} & 0 & 1350 * sin_{\theta_2} \\ 0 & 0 & 1 & 0 \\ 0 & 0 & 0 & 1 \end{bmatrix} \tag{2.6}$$

$$T_3^2 = \begin{bmatrix} cos_{\theta_3} & 0 & sin_{\theta_3} & 0.041 * cos_{\theta_3} \\ sin_{\theta_3} & 0 & -cos_{\theta_3} & 0.041 * sin_{\theta_3} \\ 0 & 1 & 0 & 0 \\ 0 & 0 & 0 & 1 \end{bmatrix} \tag{2.7}$$

$$T_4^3 = \begin{bmatrix} cos_{\theta_4} & 0 & -sin_{\theta_4} & 0 \\ sin_{\theta_4} & 0 & cos_{\theta_4} & 0 \\ 0 & -1 & 0 & 1.2 \\ 0 & 0 & 0 & 1 \end{bmatrix} \tag{2.8}$$

$$T_5^4 = \begin{bmatrix} cos_{\theta_5} & 0 & sin_{\theta_5} & 0 \\ sin_{\theta_5} & 0 & -cos_{\theta_5} & 0 \\ 0 & 1 & 0 & 0 \\ 0 & 0 & 0 & 1 \end{bmatrix} \tag{2.9}$$

$$T_6^5 = \begin{bmatrix} cos_{\theta_6} & -sin_{\theta_6} & 0 & 0 \\ sin_{\theta_6} & cos_{\theta_6} & 0 & 0 \\ 0 & 0 & 1 & 0.24 \\ 0 & 0 & 0 & 1 \end{bmatrix} \tag{2.10}$$

Using equations (2.5-2.10) all transformation matrices for all links mathematically represented. The transformation matrices for each frame with respect the base frame in the world coordinates can be found by equations (2.11-2.16).

$$T_1^0 = T_1^0 \tag{2.11}$$

$$T_2^0 = T_1^0 * T_2^1 \tag{2.12}$$

$$T_3^0 = T_1^0 * T_2^1 * T_3^2 \tag{2.13}$$

$$T_4^0 = T_1^0 * T_2^1 * T_3^2 * T_4^3 \tag{2.14}$$

$$T_5^0 = T_1^0 * T_2^1 * T_3^2 * T_4^3 * T_5^4 \tag{2.15}$$

And the final transformation from end effector to the base frame of the robot is found below,

$$T_6^0 = T_1^0 * T_2^1 * T_3^2 * T_4^3 * T_5^4 * T_6^4 \tag{2.16}$$

The transformation matrix T_6^0 is constructed by 4x4 matrix and the elements of the matrix is stated below.

$$T_6^0 = \begin{bmatrix} r_{11} & r_{12} & r_{13} & d_x \\ r_{21} & r_{22} & r_{23} & d_y \\ r_{31} & r_{32} & r_{33} & d_z \\ 0 & 0 & 0 & 1 \end{bmatrix} \tag{2.17}$$

End effector position is the 3x1 vector $[d_x \quad d_y \quad d_z]^T$. This the last column of the 4x4 homogenous transformation matrix.

For example, an arbitrary transformation matrix for the Frame 6 to base Frame can be written as follows;

$$T_6^0 = \begin{bmatrix} r_{11} & r_{12} & r_{13} & 0.65 \\ r_{21} & r_{22} & r_{23} & -0.95 \\ r_{31} & r_{32} & r_{33} & 1.8 \\ 0 & 0 & 0 & 1 \end{bmatrix} \tag{2.18}$$

In equation (2.18), the last column indicates the end effector position in the world coordinates 0.65 unit in X positive direction, 0.95 unit in Y negative direction and 1.8 unit in Z positive direction.

The orientation of the end effector is found by Roll-Pitch-Yaw (XYZ) in fixed coordinates with respect to the base frame of the robot in the world coordinates. The following equations are used to find to determine from the 4x4 transformation matrix T_6^0.

$$\begin{aligned} \beta &= atan2(-r_{31}, \sqrt{{r_{11}}^2 + {r_{21}}^2}) \\ \alpha &= atan2\left(\frac{r_{21}}{\cos(\beta)}, \frac{r_{11}}{\cos(\beta)}\right) \\ \gamma &= atan2\left(\frac{r_{32}}{\cos(\beta)}, \frac{r_{33}}{\cos(\beta)}\right) \end{aligned} \tag{2.19}$$

In the case for $\beta = \pm 90$, equations (2.19) denominator part for the $\cos(\pm 90) = 0$ therefore equations (2.20-2.21) are to be used.

If the case $\beta = +90$:

$$\alpha = 0 \; and \; \gamma = atan2(r_{12}, r_{22}) \tag{2.20}$$

If the case $\beta = -90$:

$$\alpha = 0 \; and \; \gamma = -atan2(r_{12}, r_{22}) \tag{2.21}$$

2.2 The kinematic decoupling method and Implementation for industrial robots

In this chapter, an analytical solution for forward and inverse kinematics of serial arm robot with a spherical wrist will be introduced based on kinematic decoupling proposed by Branstötter et al. study [9]. Industrial manipulators with serial 6 revolute axis have maximum 16 solutions to reach desired position and the orientation without considering the feasible limits. In the case of spherical wrist condition such that the last three axis coincides at a point, the possible inverse kinematic solutions deduced to 8, where the feasible limits of the joints are neglected. The ortho parallel term is introduced by Ottaviana et al. [41] and it can be explained kinematically by definition, the first joint of the robot is orthogonal to the second one and the third joint is parallel to the previous joint. The decoupling method proposed by Pieper [42] is takes the advantage of spherical wrist design for the industrial manipulator. This method divides the inverse kinematics problem into two sub-problems namely orientation and the positioning and proposes and relatively simpler approach for inverse kinematic solution.

Branstötter et al. [9] proposed and approach that combines the ortho-parallelism of the first 3 three joint and the spherical wrist structure of the industrial manipulators and comes with and generalized analytical solution for most of the industrial manipulator available in the market. The main advantage of the new method the parameters that required for the solution of the inverse kinematics of the industrial robots. In this approach only 7 parameters are needed, which can be gathered easily from the manufacturer specs and datasheets. The method introduced is relatively fast according to algebraic and geometrical approaches in the literature. [1], [43].

In Figure 2-8, the required parameters are shown as the arm lengths and the offsets. The world coordinate system and the end effector coordinate system are identified as $0_0 x_0 y_0 z_0$ and $0_e x_e y_e z_e$ respectively. The joint angles are defined as the $\theta_{1\ldots to\ldots 6}$. All the joints set as zero in Figure 2-8 and the parameters for Kuka KR240 R2900 are defined in Table 2-3.

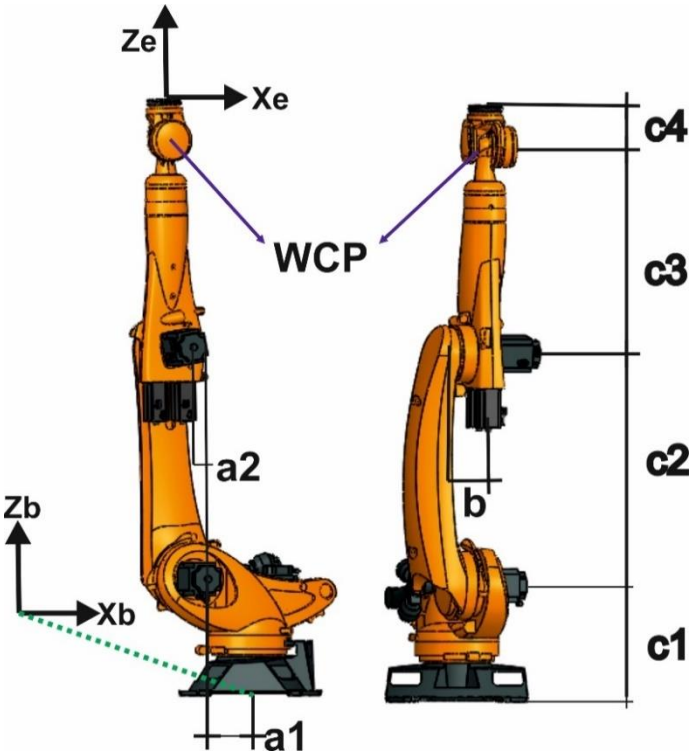

Figure 2-8: Robot parameters

a1	c1	c2	c3	c4	a2	d7
350 mm	675 mm	1350 mm	120 mm	240 mm	41 mm	0

Table 2-3: Robot parameter values

The given orientation and the position of the end effector in the base coordinate system is defined in a 3x3 rotation matrix R_e^0 and 3x1 vector u_0.

$$R_e^0 = \begin{bmatrix} e_{1,1} & e_{1,2} & e_{1,3} \\ e_{2,1} & e_{2,2} & e_{2,3} \\ e_{3,1} & e_{3,2} & e_{3,3} \end{bmatrix} \tag{2.22}$$

$$u_0 = \left[u_{x0}, u_{y0}, u_{z0}\right]^T \tag{2.23}$$

The coordinate of the spherical wrist is calculated by the following equation:

$$\begin{bmatrix} c_{x0} \\ c_{y0} \\ c_{z0} \end{bmatrix} = \begin{bmatrix} u_{x0} \\ u_{y0} \\ u_{z0} \end{bmatrix} - c_4 R_e^0 \begin{bmatrix} 0 \\ 0 \\ 1 \end{bmatrix} \tag{2.24}$$

Equation 2.24 is basically the gather the coordinate by moving the length of the c_4 in the end effector orientation from the end effector position with respect base frame.

For a certain posture of the robot there are maximum 4 different solutions obtained from the first 3 joints.

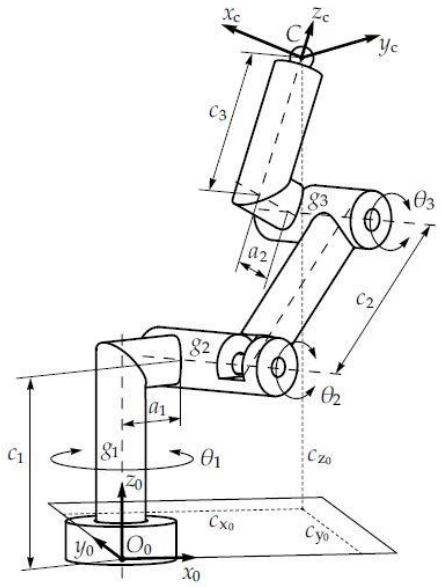

Figure 2-9: Required values of first three joints [9]

To find a solution for the forward kinematics of first 3 joints the following equations is used. The required values are given in Figure 2-9.

$$\begin{aligned} c_{x0} &= c_{x1} cos\theta_1 - c_{y1} sin\theta_1 \\ c_{y0} &= c_{x1} sin\theta_1 + c_{y1} cos\theta_1 \\ c_{z0} &= c_{z1} + c_1 \end{aligned} \tag{2.25}$$

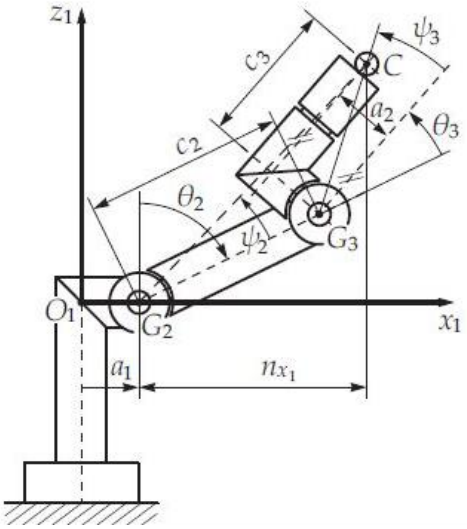

Figure 2-10: Required values of first three joint other view [9]

Afterwards the solution for the inverse kinematics of first three joints the following equations are used n_{x1} and s_1 lengths are defined below in Figure 2-10.

$$n_{x1} = c_{x1} - a_1$$

$$s1 = (c_{x1} - a_1)^2 + {c_{z1}}^2 = \sqrt{{c_2}^2 + k^2 + 2c_2 k cos(\theta_3 + \psi_3)} \tag{2.26}$$

Two possible solution for θ_3 is found by equation 2.26. The other possible solutions for inverse kinematics are found by the help of the geometrical approach. Figure 2-11 indicates the schematic view from the top for the manipulator and the available posture for Kuka Kr240 shoulder orientations.

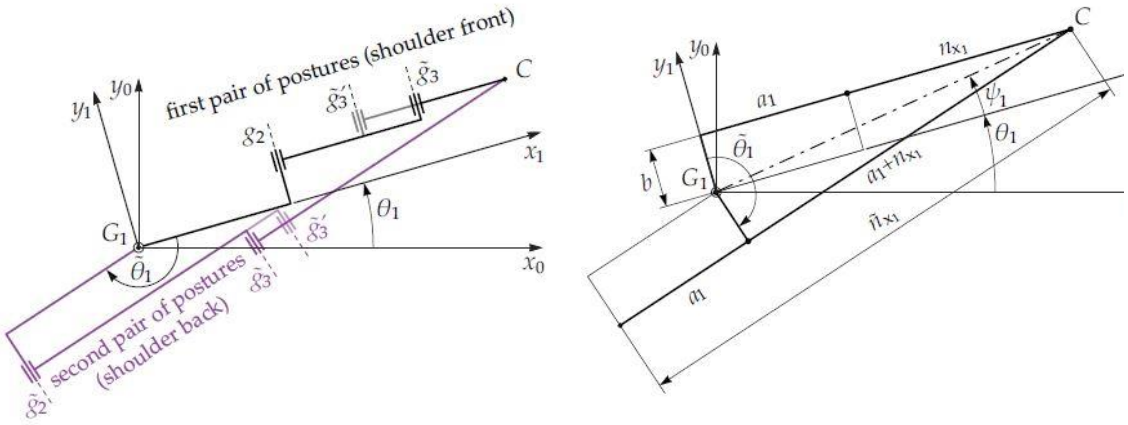

Figure 2-11: Top schematic view [9]

$$\tilde{n}_{x1} = n_{x1} + 2a_1$$
$$s2 = \sqrt{\tilde{n}_{x1}^2 + {c_{z1}}^2} = \sqrt{(n_{x1} + 2a_1)^2 + {c_{z1}}^2} = \sqrt{(c_{x1} + a_1)^2 + {c_{z1}}^2} \tag{2.27}$$

The wrist center point's (WCP) projection with respect to the z_0 axis is also determined by the following equation.

$$\psi_1 = atan2(b, n_{x1} + a_1) \tag{2.28}$$

The first joint angle calculated step by step with equations below and the notation is basically $\theta_{Axis\ No;Solution\ No}$ as follows.

$$\theta_{1;\,i} + \psi_1 = atan2\left(c_{y0}, c_{x0}\right)$$
$$\theta_{1;\,i} = atan2\left(c_{y0}, c_{x0}\right) - atan2((b, n_{x1} + a_1) \tag{2.29}$$

The second solution the first axis is determined by the followed equation.

$$\theta_{1;\,ii} = \theta_{1;\,i} - \tilde{\theta}_1 = \theta_{1;\,i} - 2\left(\frac{\pi}{2} - \psi_1\right) = \theta_{1;\,i} + 2\psi_1 - \pi \tag{2.30}$$

For the first 3 axes, the required set of equations identified to solve the positioning part of the problem.

$$\begin{gathered}
\theta_{1;i} = atan2\left(C_{y0}, C_{X0}\right) - atan2(b, n_{x1} + a_1) \\
\theta_{1;ii} = atan2\left(C_{y0}, C_{X0}\right) - atan2(b, n_{x1} + a_1) - \pi \\
\theta_{2;i,ii} = \pm acos\left(\frac{{s_1}^2 + {c_2}^2 - k^2}{2\, s_1 c_2}\right) + atan2(n_{x1}, c_{z0} - c_1) \\
\theta_{2;iii,iv} = \pm acos\left(\frac{{s_2}^2 + {c_2}^2 - k^2}{2\, s_2 c_2}\right) + atan2\left(n_{x1}, +2a_{1,} c_{z0} - c_1\right) \\
\theta_{3;iii,iv} = \pm acos\left(\frac{{S_2}^2 + {C_2}^2 - k^2}{2 C_2 k}\right) + atan2(a_2 - c_3)
\end{gathered} \tag{2.31}$$

$$\begin{gathered}
n_{x1} = \sqrt{{c_{x0}}^2 + {c_{y0}}^2 - b^2} - a_1 \\
{s_1}^2 = {n_{x1}}^2 + (c_{z0} - c_1)^2 \\
{s_2}^2 = (n_{x1} + 2a_1)^2 + (c_{z0} - c_1)^2 \\
k^2 = {a_2}^2 + {c_3}^2
\end{gathered} \tag{2.32}$$

The positioning solution held by the help of equations 2.31-2.32 the remaining axes that composing the wrist structure, Figure 2-8, that helps to orienting the end effector the desired pose following procedure is followed. For every positioning solution the other joints (the 4th 5th and 6th) need to be adapted to gathering the desired orientation for the end effector. So that the wrist center point which is described with respect to the base frame with and rotation matrix R_c^0 is has to be transformed with and another rotation matrix R_e^c that compose by the as below.

$$R_e^c = {R_c^0}^T R_e^0 \tag{2.33}$$

Matrix R_e^c contains the z_c axis rotation then the y_c axis rotation and the rotation with respect to the new z_c axis, finally the z_c constructed as the form below.

$$R_c^0 = \begin{bmatrix} \mathcal{C}_1\mathcal{C}_2\mathcal{C}_3 - \mathcal{C}_1\mathcal{S}_2\mathcal{S}_3 & -\mathcal{S}_1 & \mathcal{C}_1\mathcal{C}_2\mathcal{S}_3 + \mathcal{C}_1\mathcal{S}_2\mathcal{C}_3 \\ \mathcal{S}_1\mathcal{C}_2\mathcal{C}_3 - \mathcal{S}_1\mathcal{S}_2\mathcal{S}_3 & \mathcal{C}_1 & \mathcal{S}_1\mathcal{C}_2\mathcal{S}_3 + \mathcal{S}_1\mathcal{S}_2\mathcal{C}_3 \\ -\mathcal{S}_2\mathcal{C}_3 - \mathcal{C}_2\mathcal{S}_3 & 0 & -\mathcal{S}_2\mathcal{S}_3 + \mathcal{C}_2\mathcal{C}_3 \end{bmatrix} \tag{2.34}$$

$$R_e^c = \begin{bmatrix} \mathcal{C}_4\mathcal{C}_5\mathcal{C}_6 - \mathcal{S}_4\mathcal{S}_6 & -\mathcal{C}_4\mathcal{C}_5\mathcal{S}_6 - \mathcal{S}_4\mathcal{C}_6 & \mathcal{C}_4\mathcal{S}_5 \\ \mathcal{S}_4\mathcal{C}_5\mathcal{C}_6 + \mathcal{C}_4\mathcal{S}_6 & -\mathcal{S}_4\mathcal{C}_5\mathcal{S}_6 + \mathcal{C}_4\mathcal{C}_6 & \mathcal{S}_4\mathcal{S}_5 \\ -\mathcal{S}_5\mathcal{C}_6 & \mathcal{S}_5\mathcal{S}_6 & \mathcal{C}_5 \end{bmatrix} \tag{2.35}$$

The element [3,3] of equation (2.35) provides the joint angle of the 5th axis, the elements [1,3] and [2,3] gives the joint angle of the 4th axis similarly the elements [3,1] and [3,2] indicates the 6th joint angle. For the other possible solutions following equations are used.

$$\begin{gathered} \theta_{4;p} = atan2(e_{2,3}\mathcal{C}_{1;p} - e_{1,3}\mathcal{S}_{1;p}\,, e_{1,3}\mathcal{C}_{23;p}\,\mathcal{C}_{1;p} + e_{2,3}\mathcal{C}_{23;p}\,\mathcal{S}_{1;p} - e_{3,3}\mathcal{S}_{23;p}) \\ \theta_{4;q} = \theta_{4;p} + \pi \\ \theta_{5;p} = atan2\left(\sqrt{1 - {m_p}^2}, m_p\right) \\ \theta_{5;q} = -\theta_{5;p} \\ \theta_{6;q} = atan2\left(e_{1,2}\mathcal{S}_{23;p}\mathcal{C}_{1;p} + e_{2,2}\mathcal{S}_{23;p}\mathcal{S}_{1;p} + e_{3,2}\,\mathcal{C}_{23;p}\,, -e_{1,1}\mathcal{S}_{23;p}\mathcal{C}_{1;p}\right. \\ \left. - e_{2,1}\mathcal{S}_{23;p}\mathcal{S}_{1;p} - e_{3,1}\,\mathcal{C}_{23;p}\right) \\ \theta_{6;q} = \theta_{6;p} - \pi \end{gathered} \tag{2.36}$$

Where;

$$\begin{gathered} m_p = e_{1,3}\mathcal{S}_{23;p}\mathcal{C}_{1;p} + e_{2,2}\mathcal{S}_{23;p}\mathcal{S}_{1;p} + e_{3,3}\,\mathcal{C}_{23;p} \\ \mathcal{S}_{1;p} = sin(\theta_{1;p}) \\ \mathcal{S}_{23;p} = sin(\theta_{2;p} + \theta_{3;p}) \\ \mathcal{C}_{1;p} = cos(\theta_{1;p}) \end{gathered} \tag{2.37}$$

$$C_{23;p} = cos(\theta_{2;p} + \theta_{3;p})$$
$$p = \{i, ii, iii, iv\}$$
$$q = \{v, vi, vii, viii\}$$

All the possible solutions gathered using the kinematic procedure are listed in Table 2-4.

Joint	Solutions							
	1	2	3	4	5	6	7	8
1st	$\theta_{1;i}$	$\theta_{1;i}$	$\theta_{1;ii}$	$\theta_{1;ii}$	$\theta_{1;i}$	$\theta_{1;i}$	$\theta_{1;ii}$	$\theta_{1;ii}$
2nd	$\theta_{2;i}$	$\theta_{2;ii}$	$\theta_{2;iii}$	$\theta_{2;iv}$	$\theta_{2;i}$	$\theta_{2;ii}$	$\theta_{2;iii}$	$\theta_{2;iv}$
3rd	$\theta_{3;i}$	$\theta_{3;ii}$	$\theta_{3;iii}$	$\theta_{3;iv}$	$\theta_{3;i}$	$\theta_{3;ii}$	$\theta_{3;iii}$	$\theta_{3;iv}$
4th	$\theta_{4;i}$	$\theta_{4;ii}$	$\theta_{4;iii}$	$\theta_{4;iv}$	$\theta_{4;v}$	$\theta_{4;vi}$	$\theta_{4;vii}$	$\theta_{4;viii}$
5th	$\theta_{5;i}$	$\theta_{5;ii}$	$\theta_{5;iii}$	$\theta_{5;iv}$	$\theta_{5;v}$	$\theta_{5;vi}$	$\theta_{5;vii}$	$\theta_{5;viii}$
6th	$\theta_{6;i}$	$\theta_{6;ii}$	$\theta_{6;iii}$	$\theta_{6;iv}$	$\theta_{6;v}$	$\theta_{6;vi}$	$\theta_{6;vii}$	$\theta_{6;viii}$

Table 2-4: Solutions table

2.3 Summary

In this chapter, Denavit-Hartenberg [8] method is explained based on the necessary procedure and the rules. Then, the implementation of D-H method [8] to industrial manipulator KUKA KR240 R2900 is given. Afterwards, the method proposed by Brandsötter et. al. [9] is explained, which is a generalized analytical solution for serial arm 6 axis robot with spherical wrist. The required steps and all the necessary equations identified, explained and implemented on the very same industrial manipulator. For the both methods all the mathematical operation are taken place in to MATLAB® 2019 70 [44]

Denavit-Hartenberg method [8] is one of the most common approach to solve robotic kinematics. The D-H method requires 4 parameters for each joint and has only two rules for the assigning the frames that is rigidly attached to the links. The derivation of D-H method

[8] is not specifically constrained so that for a similar robot there might be more than one feasible D-H parameters so that D-H method [8] does not provide unique set of parameters. On the other hand, [9] enables analytical solution for a similar robot that contains serial arms and spherical wrist, which requires 7 parameters for all robot structure that have spherical wrist.

3 TOOL POSTURE OPTIMIZATION FOR ROBOTIC 5-AXIS MILLING

3.1 Introduction

The complex parts of the aerospace, naval and automotive industry with tight tolerances is one of the motivations of 5-axis milling. The advantageous of the 5-axis milling such as accessibility and contouring capability are also well known by academia and the industry. Therefore the geometry of the 5 axis milling is presented in this chapter. Then the tool axis optimization approach introduced based on the kinematics of the industrial robot.

Tool path computation is a crucial step for machining sculptured surfaces. To generate a 5-axis tool path the milling strategy and the path topology has to be determined. Afterwards the parameteres such as step length, path interval should be selected with respect to desired machining tolerance range. Once the tool path parameters set the cutter location (CL) points is generated on the surface of the part by using a CAM software NX 12 ® [45].

The coordinates system for the 5 axis milling can be described by Figure 3-1. The coordinate systems are used to represent the process geometry, mechanics and kinematics of the 5-axis milling operations. The world coordinate system (WCS) is assigned according to machine tool by mean that it is more general and does not depent on the tool, workipece (see Figure 3-1 c). The other system is compose the Feed Cross-Feed and the Normal of the tool which is called as FCN. Figure 3-1 indicates the feed, cross-feed, normal vectors and tool axis (TA). The cutter location is defined as the tool tip location with respect to the coordinates systems and cutter contact point is the point that is in contact with the actual part.

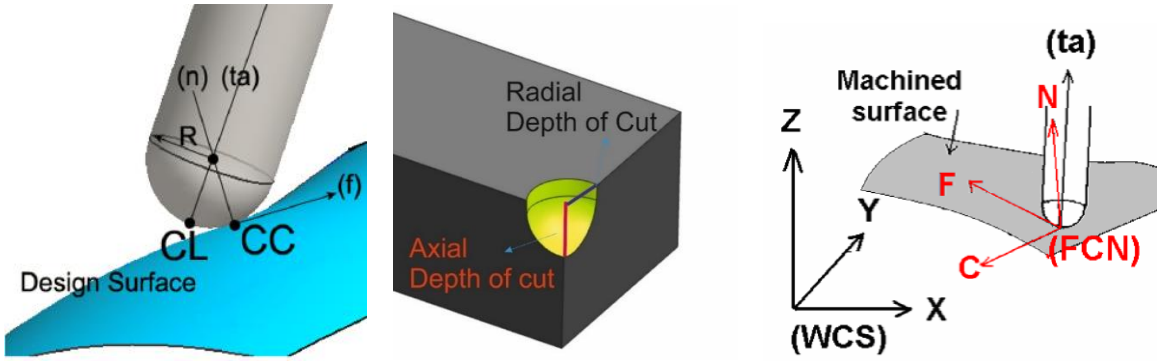

(a) (b) (c)

Figure 3-1: Multi axis milling parameters [46]

In multi axis milling the cutting tool orientation is the product of the lead and the tilt angle wixh are measured with respect to the tool axis and the surface normal of the workpiece. The lead angle is the angle between the surface normal and the tool axis about crossfeed direction. Similarly the tilt angle is measured between the tool axis and the surface normal along the feed direction. The lead and tilt angles defined with respecto the FCN coordinate sytem are identifed in Figure 3-2. The other parameter utilized for multi axis machihing is called depth of cut. To define depth of cut composed by two different geometrical aspect namely radial and axial. The depth of cuts is defined as the immersion of the cutting tool to workpiece in axial and radial direction.

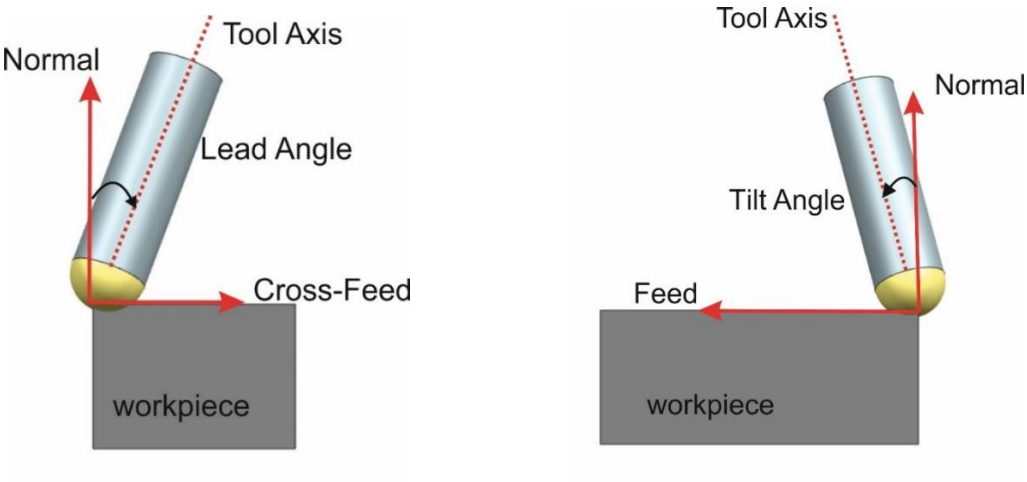

Figure 3-2: Lead and tilt angles

In this chapter the geometry of the multi-axis milling is introduced The parameters such that lead and tilt angles, cutter location (CL), tool axis (TA), cutter contact (CC) point, feed direction, cross-feed direction, and coordinates systems (FCN, WCS) are presented.

3.2 Tool axis optimization approach

Complex sculptured parts are broadly utilized in industry and multi-axis machining centers with ball end cutting tools is the prevalent approach to manufacture such shaped parts. Because of the extra DOF compared with the regular 3-axis machining tool axis selection is an involute issue for curved surfaces. It is a well-known decision parameter for manufacturing with 5-axis machining that can cause excessive amount rotary movement on the machining unit thus effects the machining quality. Therefore, in multi axis machining operations the selection of the tool axis is a crucial decision. Nonetheless, it is directly related with robot motion in a fashion of the joint angles due to articulated design of the industrial robots. In order to overcome this problem, the Dijkstra's optimization method proposed based on kinematics of 6-axis industrial robot. First, the workpiece surface properties that enables us to calculate the of the tool axis orientation and location extracted 71 [47] from the software via cutter location (CL) file of the cam software NX ®. From that CL file for each CC point the tool axis, feed, cross feed and the surface normal data extracted.

The tool axis selection directly related with the inverse kinematics of the machine tool so that selection of the tool axis arbitrarily for 5 axis milling operation can cause excessive rotations on the redundant machine tools and especially industrial robots that have a chain configuration. Therefore, the main criteria of the optimization approach is to eliminate and minimize that unnecessary rotations on the joints caused by tool axis selection. To optimize the joints motion within a range of feasible lead and tilt angles Dijkstra's shortest path algorithm used.

3.3 Dijkstra's Shortest Path Algorithm

The algorithm is first identified by the computer scientist Edsger Dijkstra in 1959. Dijkstra's algorithm is a search-based algorithm that finds the length for a shortest path of a given graph

for each vertex. The shortest path problem can be defined by $G = \{V, C\}$ where V is the vertices of the route and the C is the cost/length/weight variable of the route between vertices visualized to Figure 3-3. The vertex numbered from 1 to 11 and the route cost identified as c1 to c13 and the algorithm provides the minimum cost route from vertex 1 to 11.

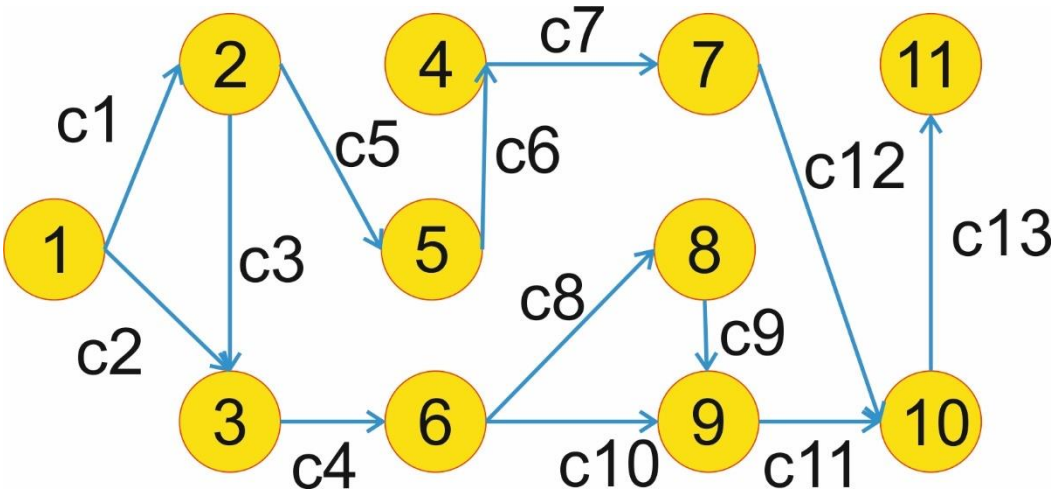

Figure 3-3: Ex. Dijkstra's path

The algorithm is calculating the minimum cost distance from a start vertex to end vertex it is also possible calculate to every combination of start/end vertex. For example the shown path in Figure 3-3 defines the possible routes from vertex 1 to 10 with the variable costs that can be the distance, time, etc. and comes with a solution by using Dijkstra's algorithm to reach vertex 11 starting from vertex 1. In this thesis the shortest path MATLAB function [48] is used for determining the optimized tool axis variation by considering the kinematics of the robot. The MATLAB® function that utilized of optimization required three parameters namely the source target and weight from the source to target. Equation (3.1) is demonstrated to perform function.

$$source = [1\ 1\ 2\ 2\ 3\ 5\ 4\ 6\ 6\ 9\ 7\ 11]$$
$$\text{target} = [2\ 3\ 3\ 5\ 6\ 4\ 7\ 8\ 9\ 11\ 11\ 10] \quad (3.1)$$
$$\text{weight} = [c1\ c2\ c3\ c5\ c4\ c6\ c7\ c8\ c10\ c11\ c12\ c13]$$

Equation 3.1 defines the source matrix and target matrix according to the routes that shown in Figure 3-3.

3.4 Implementation of Dijkstra's Algorithm to 5-axis Milling

In this implementation of the Dijkstra's shortest path algorithm to 5-axis milling toolpath is defined. Apart from the name the algorithm is implemented to determine optimal variable tool axis for a predefine tool path. Thus, the predefined tool path has the same length before and after the optimization. The main goal of the proposed algorithm in this thesis to determine the optimal tool axis selection on the CL points. Therefore, the required adaptations are done for Dijkstra's shortest path algorithm which are defining possible cutter contact points as vertex. The routes between each vertex through the feed direction defined as the cost to the algorithm. Figure 3-4, represents the tool path and defined CC points with the cost of every routes.

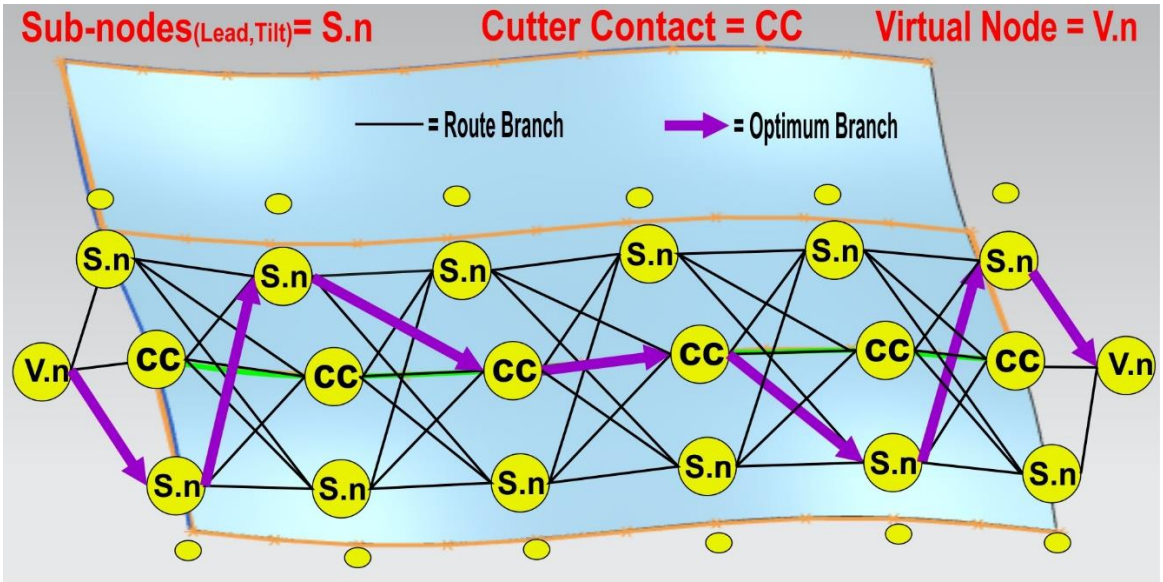

Figure 3-4: Shortest path for tool axis optimization

In Figure 3-4, CC points and Sub-nodes for a every point are defines so that tool orientation is different in every sub-node. The list view of this graph is introduced in Table 3-1. For this case the feasible lead and tilt angles minimum 0 and maximum 10 degrees therefore, the Table 3-1 constructed with lead and tilt increment as 1 degree as below for a 6-point tool path. The increment directly effects the number of sub-nodes for each particular CC point on the surface. In Figure 3-4 all possible routes between sub-nodes are visualized. The cost function is defined to the algorithm as joint angles of the robot to travel between two consecutive CL nodes. And the shortest path algorithm is searched for the minimum rotation angles of the joints while following the defined path continuously.

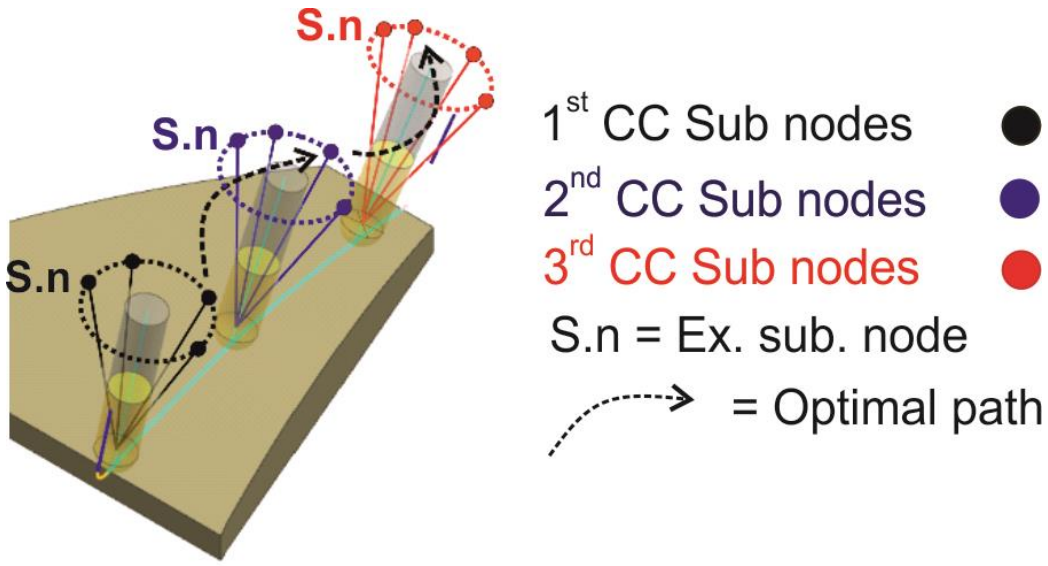

Figure 3-5: Example optimal path selection [19]

Figure 3-5 is visualized the possible sub-nodes in a different perspective for a 3 CL points predefined tool path. The colored dots represent the sub. nodes on the CL points of the surface and each possible transformation between the sub. nodes for each consecutive CL points is defined as route Figure 3-4.

Point 1	Point 2	Point 3	Point 4	Point 5	Point 6
Sub-node 1: Lead:0 Tilt:0	Sub node 1: Lead:0 Tilt:0	Sub node 1: Lead:0 Tilt:0	Sub node 1: Lead:0 Tilt:0	Sub node 1: Lead:0 Tilt:0	Sub node 1: Lead:0 Tilt:0
Sub node 2: Lead:0 Tilt:1	Sub node 2: Lead:0 Tilt:1	Sub node 2: Lead:0 Tilt:1	Sub node 2: Lead:0 Tilt:1	Sub node 2: Lead:0 Tilt:1	Sub node 2: Lead:0 Tilt:1
⋮	⋮	⋮	⋮	⋮	⋮
Sub node 56: Lead:5 Tilt:6	Sub node 56: Lead:5 Tilt:6	Sub node 56: Lead:5 Tilt:6	Sub node 56: Lead:5 Tilt:6	Sub node 56: Lead:5 Tilt:6	Sub node 56: Lead:5 Tilt:6
⋮	⋮	⋮	⋮	⋮	⋮
Sub-node 100: Lead:10 Tilt:10	Sub-node 100: Lead:10 Tilt:10	Sub-node 100: Lead:10 Tilt:10	Sub-node 100: Lead:10 Tilt:10	Sub-node 100: Lead:10 Tilt:10	Sub-node 100: Lead:10 Tilt:10

Table 3-1: Shortest path sub-nodes table

In order to stick to continuous 5-axis machining, the algorithm modified by following rules such that the routes always follow in the feed direction along the tool path. Every point defined on the surface has to be visited. And no internal loops allowed between the sub-nodes. These rules are visualized in Figure 3-6, Figure 3-7 below.

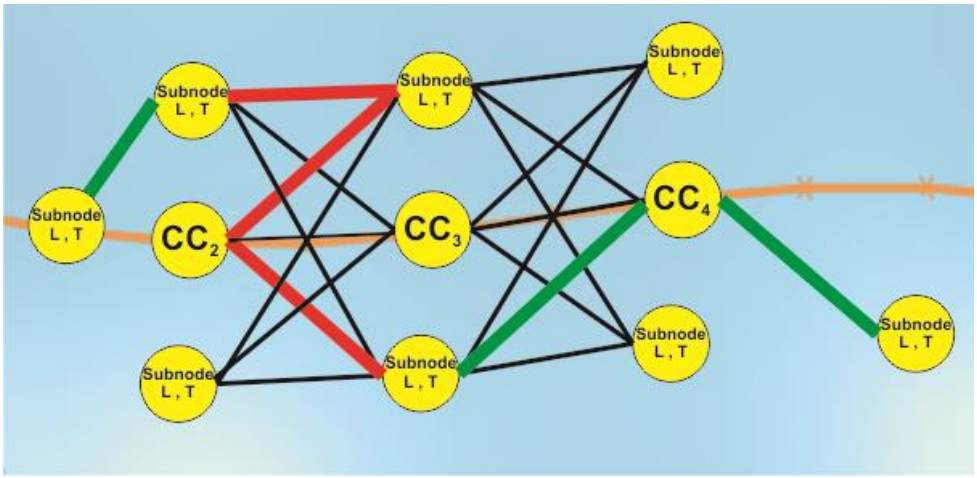

Figure 3-6 :Feed direction Violation

There is a possibility to go backwards while calculating the shortest path, however it will violate the machining approach.

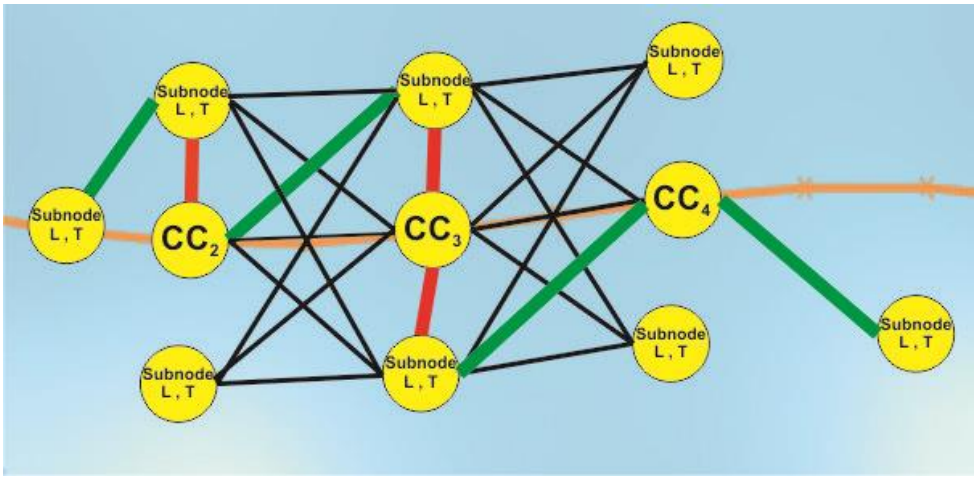

Figure 3-7: Internal looping

In Figure 3-7, he internal loop case identified, the possibility of the looping on the same point is prohibited in the algorithm.

The optimization algorithm requires the inputs such as surface data, tilt and lead angle range defined by user. If there is some special situations such specific lead and tilt angles in a certain portion of the workpiece it is also possible to define specifically to certain CL points on the workpiece. Afterwards the Dijkstra's algorithm is calculating the optimum lead and

tilt angle combination for every point. Then the optimized tool path simulated in the cam software. Finally, the optimized tool axis data is gathered.

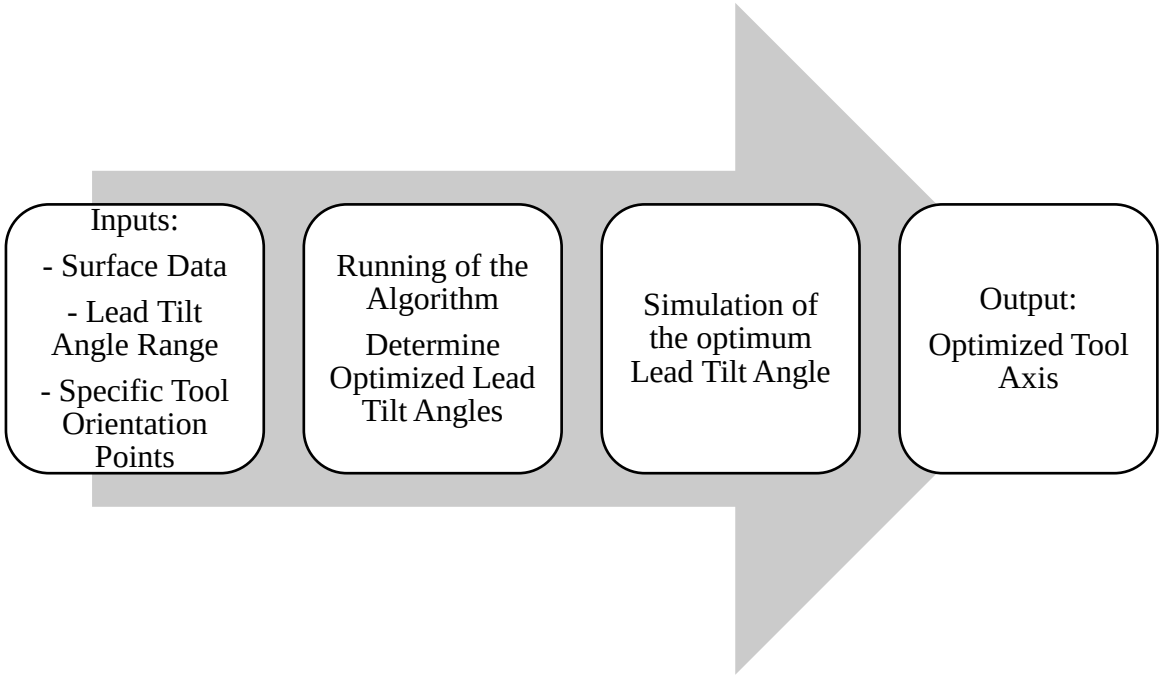

Figure 3-8: Flowchart of the algorithm

3.5 The Case Study of the Tool Axis Optimization Approach

The tool axis optimization approach is validated by a case study for a predefined single cutting step on a sculptured surface 5-axis milling. In order to simulate a real machining scenario specific CL points on the surface has a constant lead and tilt angles. In this case study the CL point 20 to 30 is set to have tool axis by lead 0 and tilt 10 degrees wrt surface normal. According to that 4 case studies are conducted.

Case 0: Constant tool axis selection (Lead=5 Tilt=10 wrt surface normal)

Case 1: Optimization of tool axis by considering the minimization of the first three axes

Case 2: Optimization of tool axis by considering the minimization of the last three axes

Case 3: Optimization of tool axis by considering the minimization of all 6 axes

The lead and tilt angle range specified as minimum -5 and maximum 10 degrees and min -5 and maximum 15 degrees respectively wrt surface normal. The search increment is select as

1 degree. The optimized tool axis and relevant lead and tilt axis are demonstrated in Figure 3-9 to Figure 3-11 for each case. The lead tilt optimization for the cases are demonstrated in the following figures.

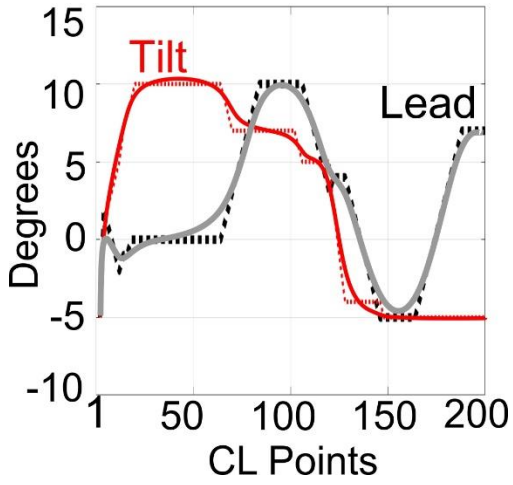

Figure 3-9 Lead and tilt angles for case 1

Case 1 is investigated the selection of the tool axis by considering the minimization of rotation of first three axis of the industrial robot. The tilt angle varied between 0 to -5 degrees and the maximum tilt went up to 10 degrees while the limit were 15 degrees. The lead angle varied between -5 to 10 degrees. (See Figure 3-9)

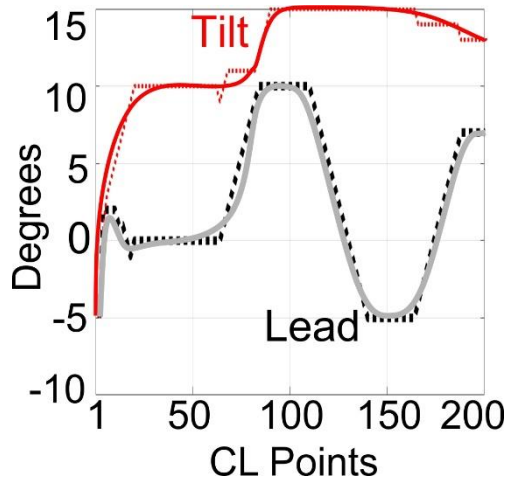

Figure 3-10: Lead and tilt angles for case 2

Case 2 is investigated the tool axis selection with respect to last three axis. The tilt angle is varied between -5 to 15 degrees. The lead angle is varied between -5 to 10 degrees and shown the similar shape.

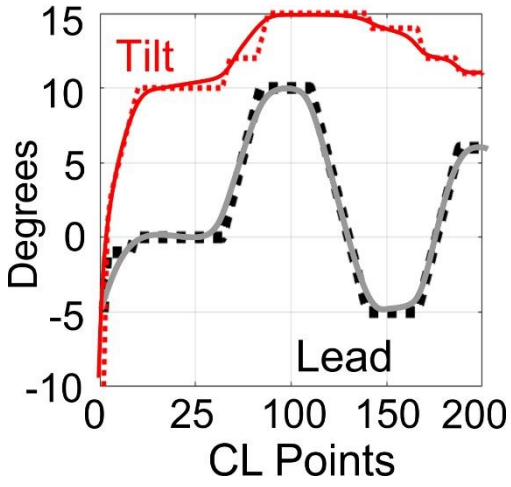

Figure 3-11 Lead tilt angles for 3

Case 3 is investigated on the tool axis selection by considering minimization of all axes of industrial robot. The lead angle started with -10 degrees and increased up the maximum limit. The lead angle starts with -5 degrees and went up to maximum then decreased to minimum limit and finished the tool path with 6 degrees.

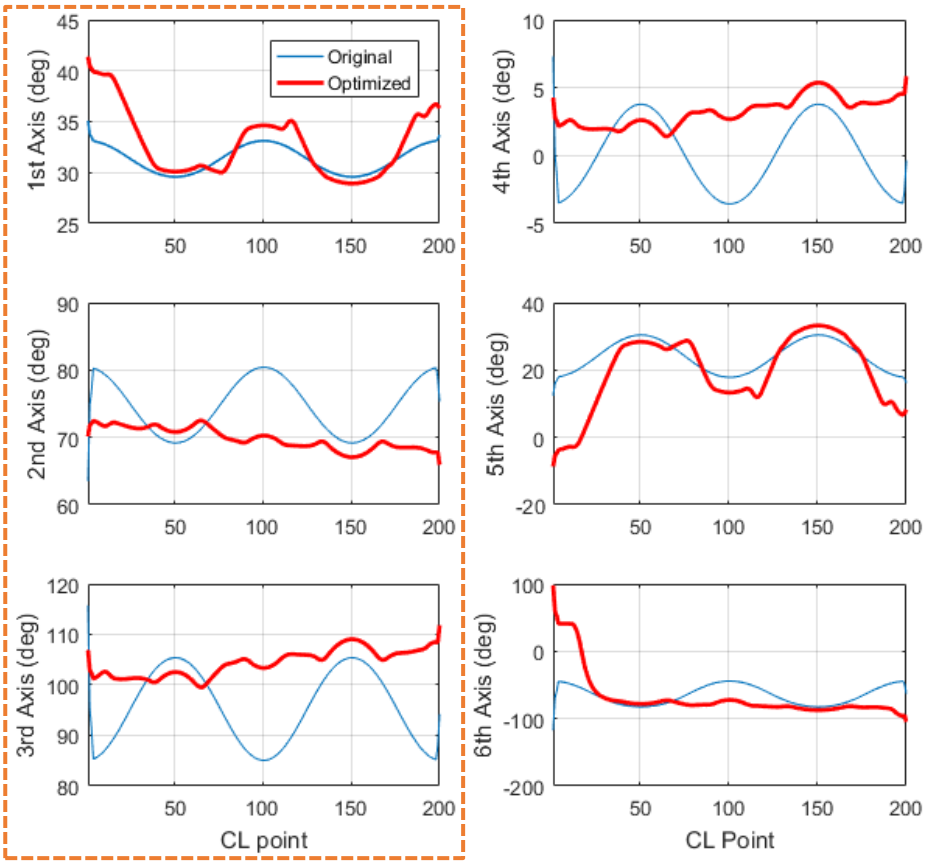

Figure 3-12: Optimized angles wrt first three axes (Case 1)

Figure 3-12 is demonstrated the optimized joint angles, the objective is to minimize the first three joints rotary movement. As can be seen in the above red lines indicates the optimized rotary movement blue lines utilized as for non-optimized rotary movement respectively case 0 and case 1.

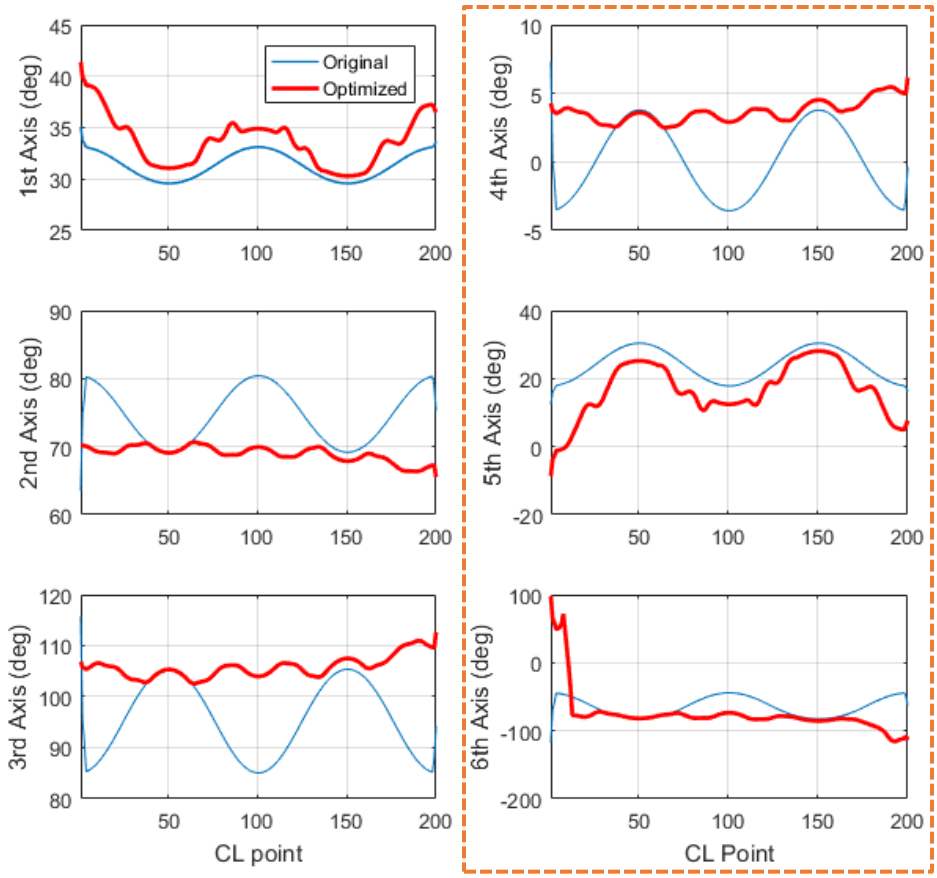

Figure 3-13: Optimized angles wrt last three axes (Case 2)

Figure 3-13 is demonstrated that optimized joint angles, the objective is to minimize the last three joint rotary movement. As can be seen in the above figure optimized and original angels in red and blue lines respectively.

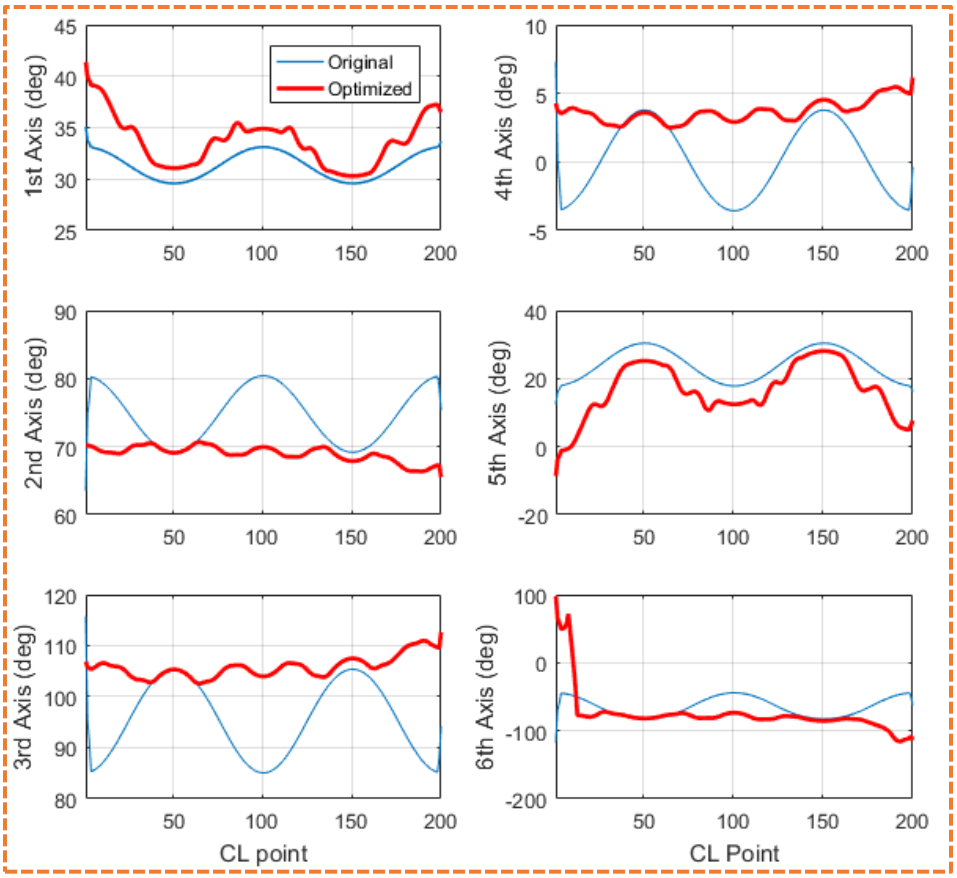

Figure 3-14: Optimized angles wrt to all axis (Case 3)

Figure 3-9 to Figure 3-11 are indicated the variation of the lead and tilt angles and for the all cases. The rotational cost is reduced significantly around 20-30 % with respect to constant tool axis selection namely 5 degrees lead and 10 degrees tilt wrt surface normal. On the other hand, the cost reduction does depend on the workpiece surface feasible range of lead tilt. The algorithm sticks to predefined rules such as feed direction, not internal looping and continues machining.

3.6 Summary

In this section the introduction for 5-axis milling is given and parameters for 5-axis milling and coordinates systems are identified. Afterwards, Dijkstra's shortest path algorithm is presented and then implementation of Dijkstra's algorithm to 5-axis tool axis selection is introduced. Optimum tool axis selection procedure is introduced in a case study for a single cutting step 5-axis milling tool path. The rotational angle differences of the joint between

two consecutive CL point is identified as cost to the shortest path algorithm the algorithm searched for the minimum cost for a tool path. The lead-tilt angles variation and the optimized joint angles are presented in Figure 3-9Figure 3-14. KUKA KR240 R2900 used as the machine tool along the optimization algorithm. The results showed that the optimization of the tool axis can deduct the unnecessary motion of the industrial manipulator up to 30% percent.

On the other hand, the robot axes drive limits is not considered such that velocity, acceleration-deceleration capabilities and positive-negative jerk limits. These limits and the achievable commanded axes rotations are highly dependent. So that, during a machining operation violation of these axis properties can cause to emergency stops, lower path accuracy and increased wear on the robot. Also, the high jerky motions can cause on the actuator wear. As a consequence, axes drive limit should be taken in to account for more smother movement and lower tracking errors and better surface quality for especially finishing operations.

4 WORKPIECE LOCATION SELECTION BASED ON ROBOT KINEMATICS

4.1 Introduction

Workpiece placement with respect to machine tool base is a crucial decision for 5-axis machining operations. The workpiece location generally selected by the NC programmer or manufacturing engineer tediously. Nonetheless this selection may cause excessive cycle time and air-time due excessive rotations also accuracy issues arising from the machine tool axis usage. It is also known that the cycle time on the software simulation is different than the actual operation time and the time difference depends on also the selection of the workpiece location.

The selection of the workpiece for 5-axis machining unit is requires experience and optimization research even for a relatively small worktable size. On the other hand, industrial robots have greater size of worktable and dexterous working volume so that it must be taken into account. Figure 4-1 is showed that the example workpiece position on work table.

(a) Workpiece positioning for 5-axis CNC unit

(b) Workpiece positioning for Industrial Robot

Figure 4-1: Ex. Workpiece locations

In this chapter the method is presented to minimize the rotary motion of the robot's first three axis. The analysis approach and the simulations introduced then the consequences of the workpiece location on the work table discussed.

4.2 Analysis approach for selection of the workpiece location

The workpiece location on the worktable is analyzed by considering the total rotary movement of the joints as a criterion. It is aimed to minimize the rotary motion of the joints for defined tool path. For such a reason, the inverse kinematics problem of the robots solved for a given tool path by iteratively changing the location of the tool path on the worktable. Therefore, the worktable divided in to equal regions.

In order to analyze the effect of the workpiece positioning on the robot kinematics. First the inverse kinematics problem solved. This step is repeated for each region on the work table.

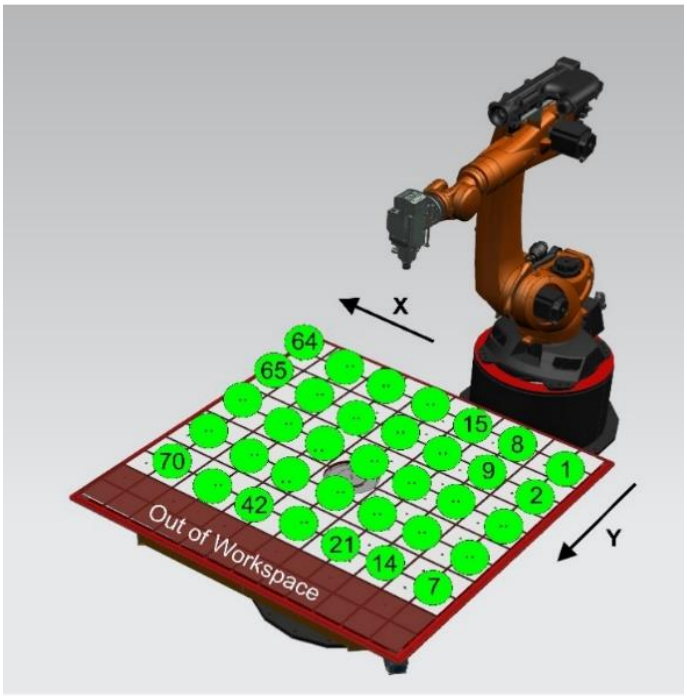

Figure 4-2: Worktable regions

The worktable divided in to equal regions (see Figure 4-2) by using the bound box of the tool path as criterion basically the feasible workspace of the robot on the worktable divided in to

bound box of the tool path. Therefore, the X axis divided in to 10 equal region Y axis divided in to 7 equal regions. In total the worktable is divided in 70 equal regions. The cost defined as the angles covered to reach consecutive CL points to complete a tool path in analyze approach. In this approach best workpiece location by considering kinematics requires inputs such as toolpath bound-box size, X and Y axes range on the worktable. Then calculates total axis rotation cost starting from the first point on the tool path.

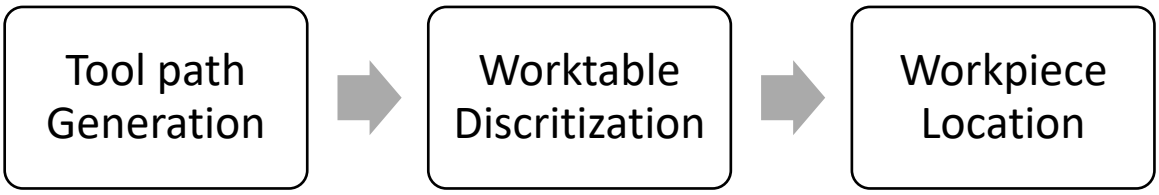

Figure 4-3: Flowchart of the workpiece location optimization method

4.3 Simulations

The simulations are organized in four different case scenarios. As a first step, the tool path generated with constant lead and tilt angles with respect to surface normal. Next the first and second case constructed regarding with the constant lead and tilt angles for feed direction X and Y respectively. The third case selected as the same tool path with varying tool axis for the feed direction X. In the 4th case study the cutting pattern selected as follow periphery. For all these case studies are analyzed and the profitable location the workpiece on the table are discussed. In the case studies the first 3 axis are investigated. Due to serial structure of the robot first three joints are highly effective on the other axes of the robot and possible accuracy errors directly effect the overall performance of the process due to leverage effect caused from the relatively long length of the 2nd and 3rd axes.

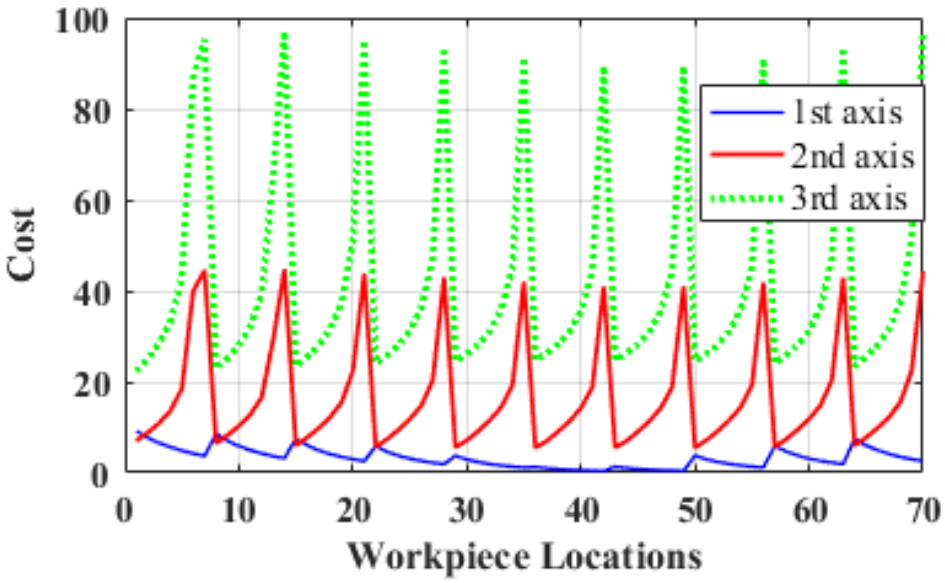

Figure 4-4: Cost evaluation for cutting direction X

For the case 1 Figure 4-4 indicates that the selection feed direction along the X axis in the machine tool coordinates. For the first axis of the robot is highly related the overall motion when the feed direction along the X axis. So that the following figure is used describe overall feasibility study for the first case scenario. The first axis' feasible region is the indicated by Figure 4-5 as outer region. The leverage effect due to serial structure of the robot decreased the usage of the 1st joint at the highlighted area. For the 2nd and 3rd axis usage the feasible area is identified to the closer of the robot on the worktable (see Figure 4-5). For an overall worktable feasibility, the mid-range is selected as a most profitable region. On the other hand, the exact center location for the worktable not the most profitable region for this cutting operation performed on the feed direction X it is more beneficial to consider place the workpiece on the use middle and slightly right-hand side. In Figure 4-4 X, around the region 40.

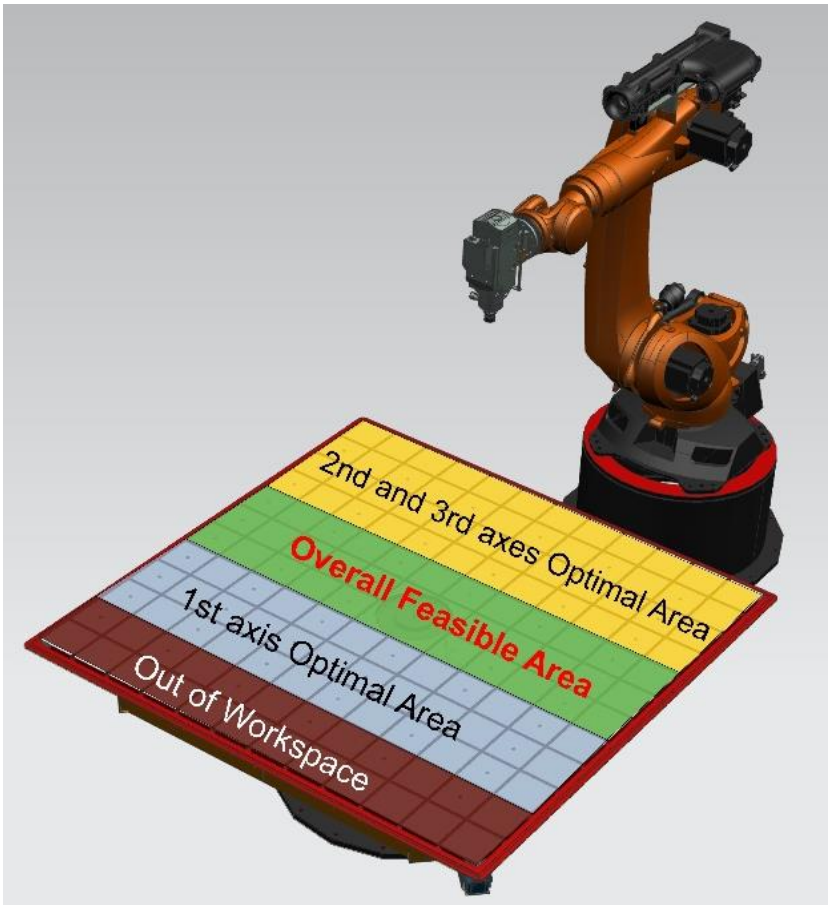

Figure 4-5: Region evaluation for cutting direction X

For the second case the feed direction is selected as the Y direction and it is observed that the for-feed direction Y, the robot's motion mostly depends on the 2nd and 3rd axes of the robot to manipulate the spindle along the Y direction. It is observed that the selection of the workpiece has diverse effect on the axes usage and figure proves that the selection of the workpiece on the distant regions with respect to X direction on the workpiece especially region between 1 to 10 and 60 to 70 in Figure 4-6.

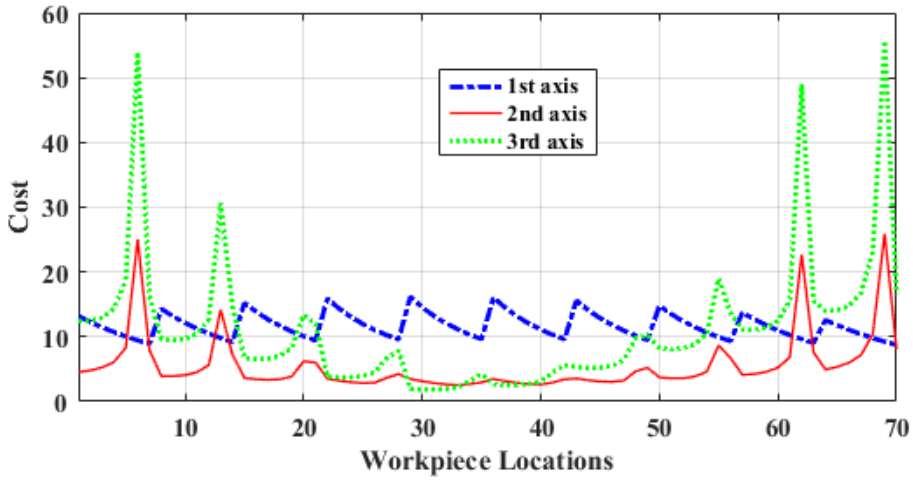

Figure 4-6: Cost evaluation for cutting direction Y

For second case the cutting direction selected as Y. Figure 4-7 is presented the optimal areas regarding to joints. For the first joint the yellow labeled areas selected as feasible region. On the other hand, the turquois region selected as optimal for the second and third axes

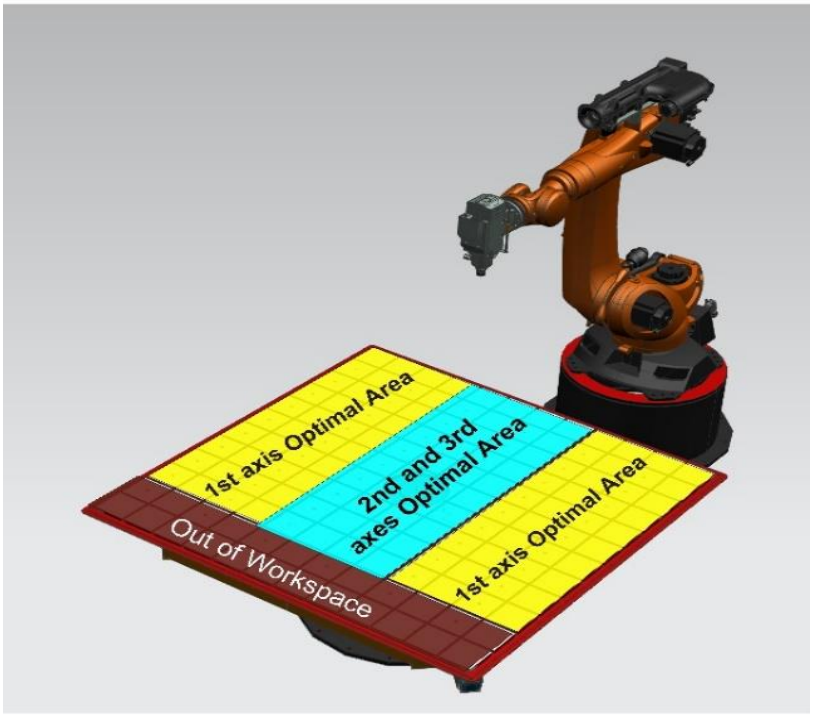

Figure 4-7: Region evaluation for cutting direction Y

The case 3 is investigated the variable tool axis tool path on the feed direction X and in this case, it is observed that for the 2nd and 3rd axes have a cyclic effect with along the Y direction therefore the to select a feasible region for workpiece first the selection should be done the along the X direction afterwards along the Y direction. And for this particular case the 30th region is selected as the most feasible are to attach workpieces. (see Figure 4-8)

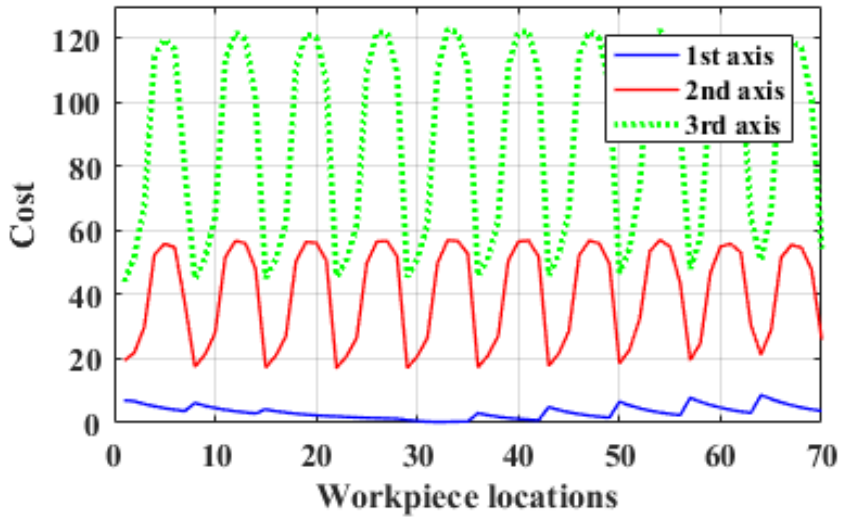

Figure 4-8: Varying tool axis cost evaluation

In the last case scenario, the tool path shape is investigated the tool path constructed by the follow periphery (contour parallel) shape. To explain better Figure 4-9 is shown in figure that consist the tool path on the surface.

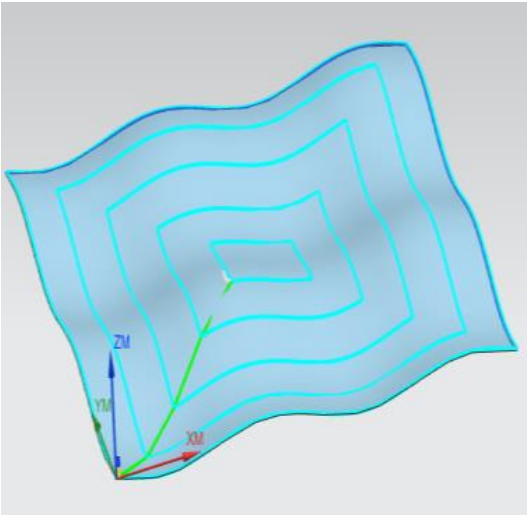

Figure 4-9: Contour parallel tool path

The contour parallel shape basically contains the feed direction in X and Y axis along the tool path. Therefore, the results indicated that all effects on the case 1 and case 2. For this case the feasible workpiece location with respect to the first axis is the center along X direction of the table. To combine with the second and third axes the inner region must be selected as an overall feasibility for the attach workpiece. The outer marginal regions are not feasible with respect to the second and third axes. (see Figure 4-10)

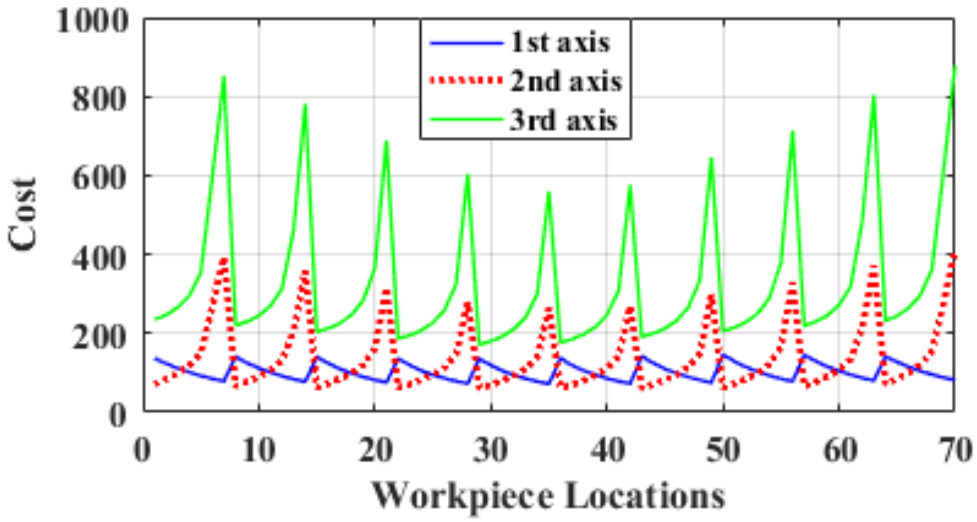

Figure 4-10: Contour parallel tool path cost evaluation

As a guideline from the insight of the case studies, with respect to the feed direction selection, the motion of robot varies. So that as a first step the feed direction should be selected. Afterwards by checking the axes rotations with each region on the worktable. According to cyclic or increased rotations, selection of the most favorable place should be determined with respect to each axis. If there are more than one region for each particular axes the selection should be done by the priority of the axis that is chosen by CAM programmer.

4.4 Summary

In this section the method introduced to optimization of the workpiece positioning of the worktable. The KUKA KR240 R2900 industrial manipulator used as a machine tool to perform 5-axis milling analysis. Robotic milling operation has a large workspace volume with respect to conventional CNC machines so that it requires to determine feasible region on the worktable. So that the case studies are performed to find a feasible region on the worktable. Rotary angles that covered between two consecutive CL points by the first 3 joints are defined as cost and calculated for an ordinary 5-axis tool path in different scenarios. Result indicates that the smooth and continuous tool path the selection of the work piece is crucial and the cutting pattern, tool axis, feed directions are identified the most important parameters. All these case studies showed that the by choosing a feasible region to attach the workpiece can reduced unnecessary rotary movement up to 4 times.

5 CONCLUSION AND FUTURE WORK

Modern advanced manufacturing industries rely on robot in different applications such as material handling, assembly, welding, cladding, spray painting and machining. Ongoing improvements in machining applications demonstrate the significance of flexibility for compelling machining. However, utilization of industrial robots for machining applications is a rising approach for the most recent decades. Particularly for large scale parts that requiring moderately less precision for example composites. On contrary only 5% of the robots assigned to material removing operations such as deburring etc. In such manner utilization of the robots for milling tasks is generally constrained. On the other hand, industrial robots have advantageous with respect to conventional CNCs such that reconfigurability, foot print ratio to working space, kinematic flexibility, low capital investment.

The increasing complexity of the industry with tighter tolerances are solid motivations for multi-axis milling operations continuously growing. 5-axis milling is mostly utilized in the machining sculptured surfaces, turbine blades, impellers which offers better accessibility with the help of increased tool axis orientation capability by lead and tilt angles. Industrial robots that offering 6 DOF motion capability provides one redundant axis for 5-axis milling applications which requires to investigation considering the robot kinematics and dynamics. Therefore, in this thesis an approach proposed to determine optimum tool orientation along the predefined tool path. In the optimization method, it is aimed to minimize axis rotations of the industrial robot by specifying the optimal lead and tilt combination for every CL point. Dijkstra's shortest path algorithm utilized, and the cost function identified as the rotations angles between CL points. In 5-axis milling, tool axis selection directly effects the motion of the robot due serial kinematic chain so that main goal is the eliminate excessive rotations sourced from the in proper selection of the tool axis. Dijkstra's algorithm searches for the minimum cost route by calculating every lead and tilt combination for each CC point sub nodes. Even such a small cutting step composed of 100 to 200 CC point, possible lead and

tilt combination between the sub nodes are more than 10 million. Also, this number depends the lead tilt feasible range and the increment. The case study is conducted to demonstrate for a tool path and results showed that the rotational cost can be decreased around 30% with respect to an arbitrary constant tool axis.

Workpiece position with respect the machining unit base is a critical decision in 5-axis machining and effects surface quality and machining tolerances. For robotic milling is also vital because of the serial structure of the robot workpiece location have a direct effect on the axis usage. It is also known that the cycle time on the CAM interface different than the actual cycle time due to redundant rotations. Therefore, randomly chosen workpiece location can cause excessive cycle time and accuracy issues due to unnecessary movement of the machine tool axis. Thus, the effect of the workpiece location is analyzed by taken into account of the total rotary movement for particular axes. In this study the first three axes rotary movement utilized as a metric. The worktable divided into regions by using the bound box of the tool path. In each region the inverse kinematic problem solved, and the axis rotational cost evaluated with a case study and results indicate that the optimal positioning of the workpiece can deduce the rotational cost up to 4 times, leading to potential accuracy improvement.

As a future work the kinematic model can be merged with the axis velocity and jerk profile and the optimal tool axis and workpiece location can be evaluated with that knowledge. In addition, with the stiffness model of the robot the overall optimization scheme can be constructed for the same criteria and overall performance and productivity of the robot can be assessed.

In this thesis a kinematic model of the robot is developed. The Dijkstra's optimization algorithm utilized to determine optimal tool axis selection along a tool path. Also, the workpiece positioning by considering the robot kinematic. These were not present in the literature. It is observed that the optimization methodologies and the criteria can be extended and improved.

7 APPENDIX

In this chapter the following procedure explained in order to use the industrial robot Kuka KR240 as a machine tool. The robot is installed to the Cam software Siemens NX® library by the following steps. The steps and the required adaptations visualized by Figure 7-1 Figure 7-13.

As a first step the robot 3D CAD data gathered from the manufacturer's website. Afterwards with help of the manufacturing module of the CAM software the robot is identified as a machine tool that is able to execute a G-code and all related features as a machine tool. The following steps are used to identify all the operation.

As a first step the machine base and robot base are identified then all the axis and the joint types assigned respectively from 1-6. The name of the axes are defined as A1 to A6 and the junction the axes are defined A1_JCT to A6_JCT. Afterwards the spindle that attached to the 6th-axis of the robot added to machine tool tree.

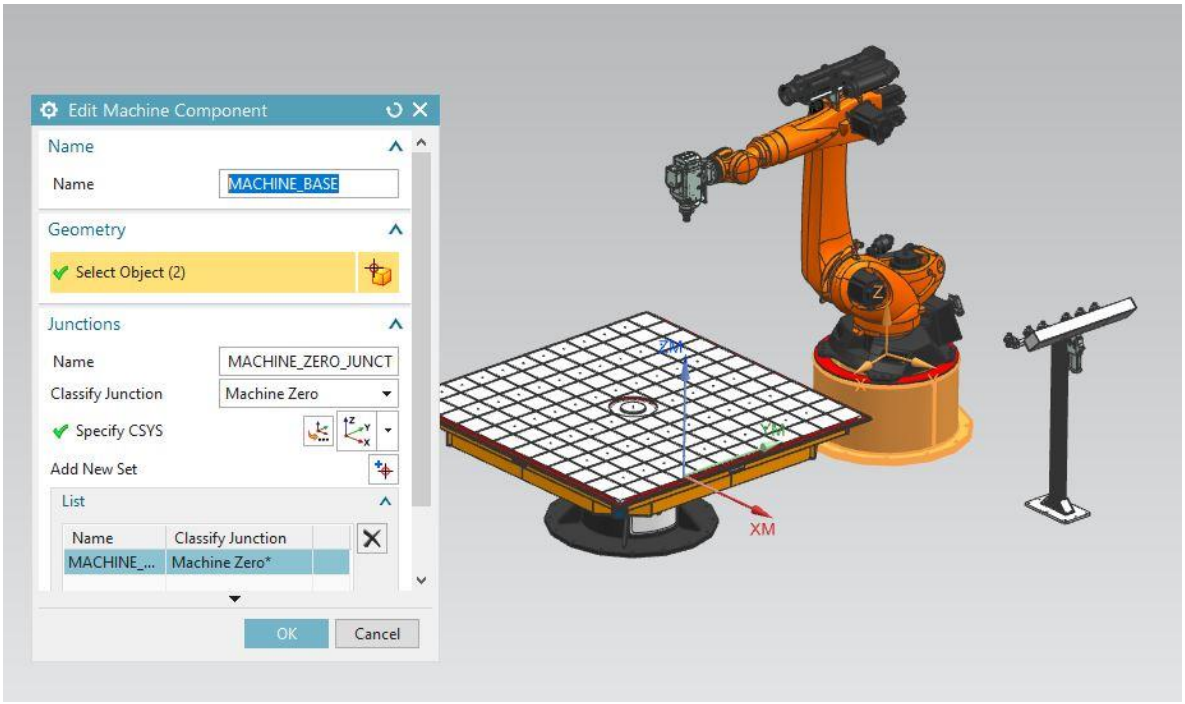

Figure 7-1: Machine base

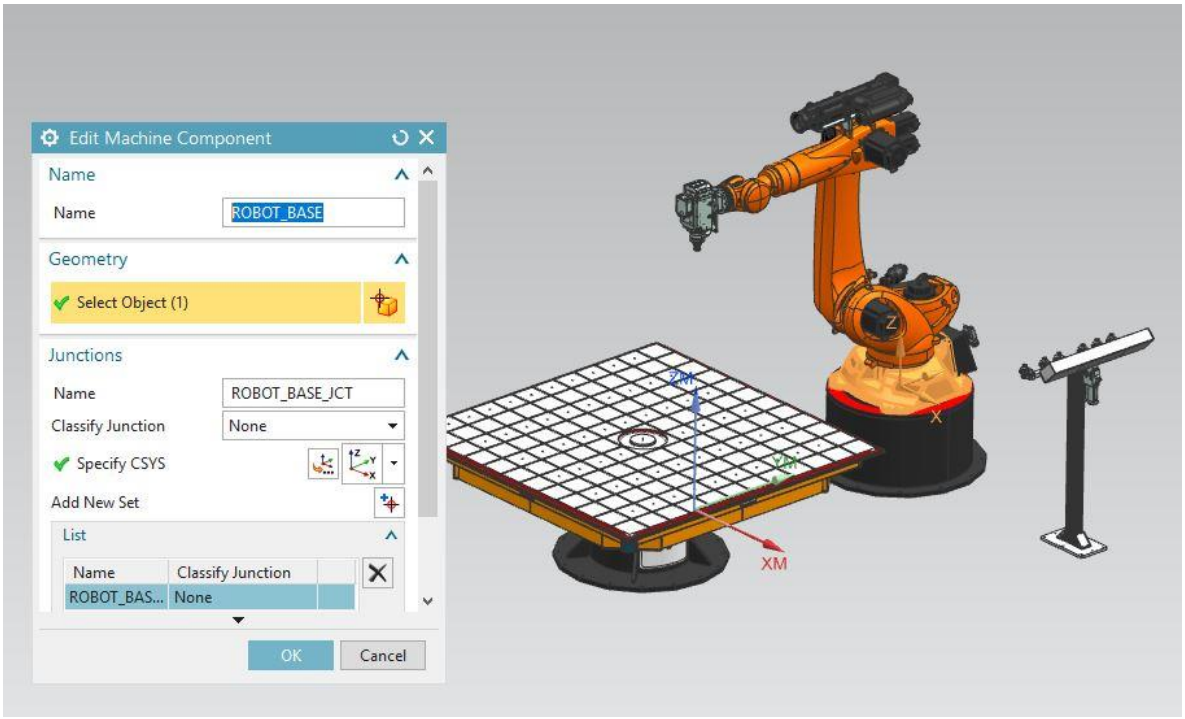

Figure 7-2: Robot base

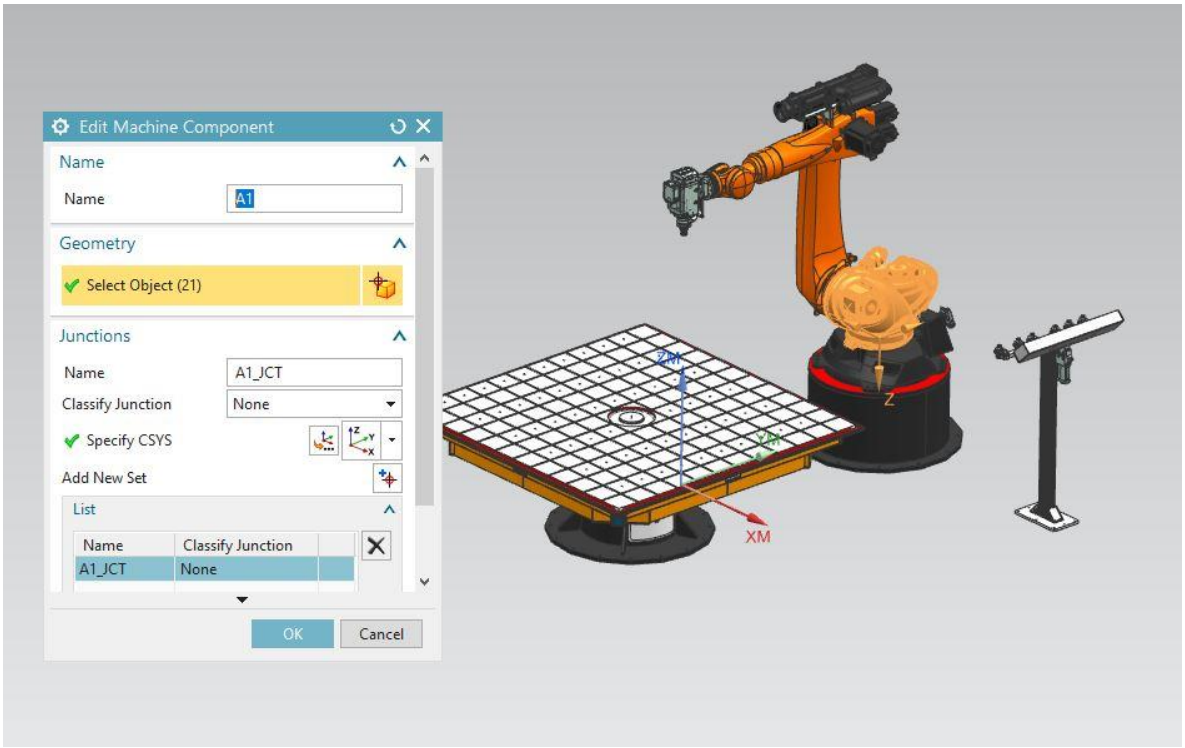

Figure 7-3: First axis

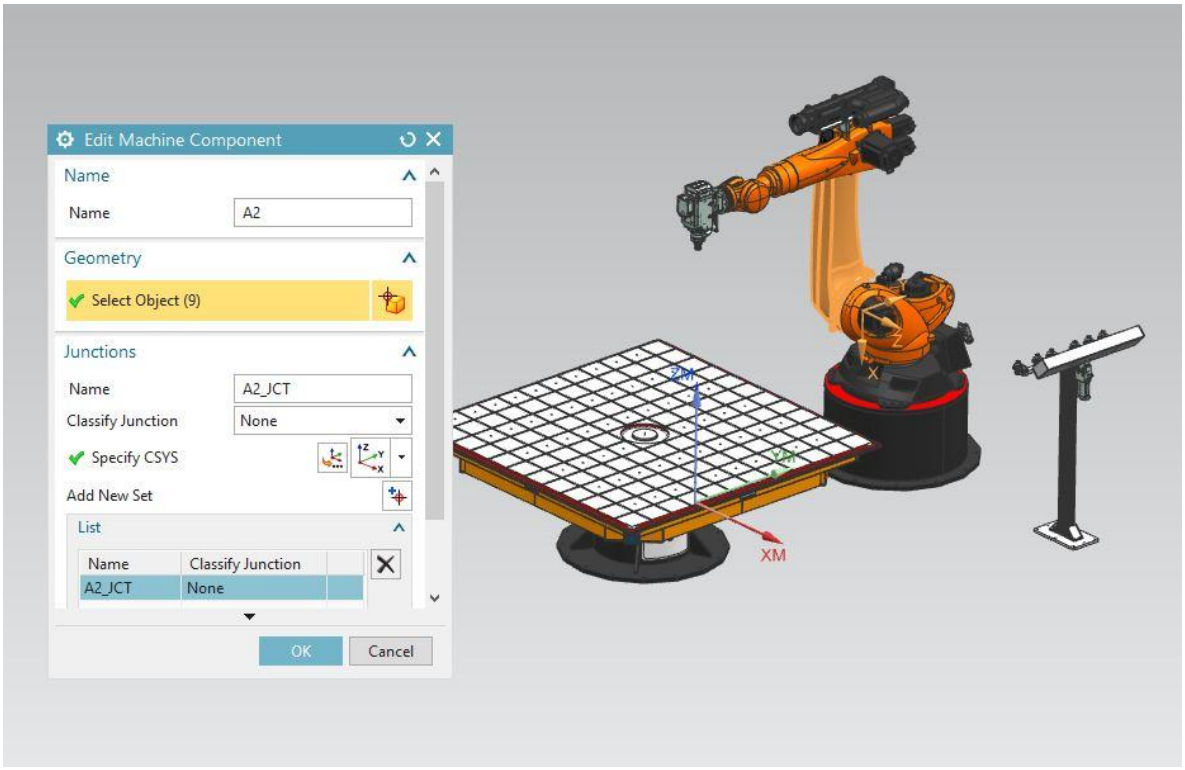

Figure 7-4: Second Axis

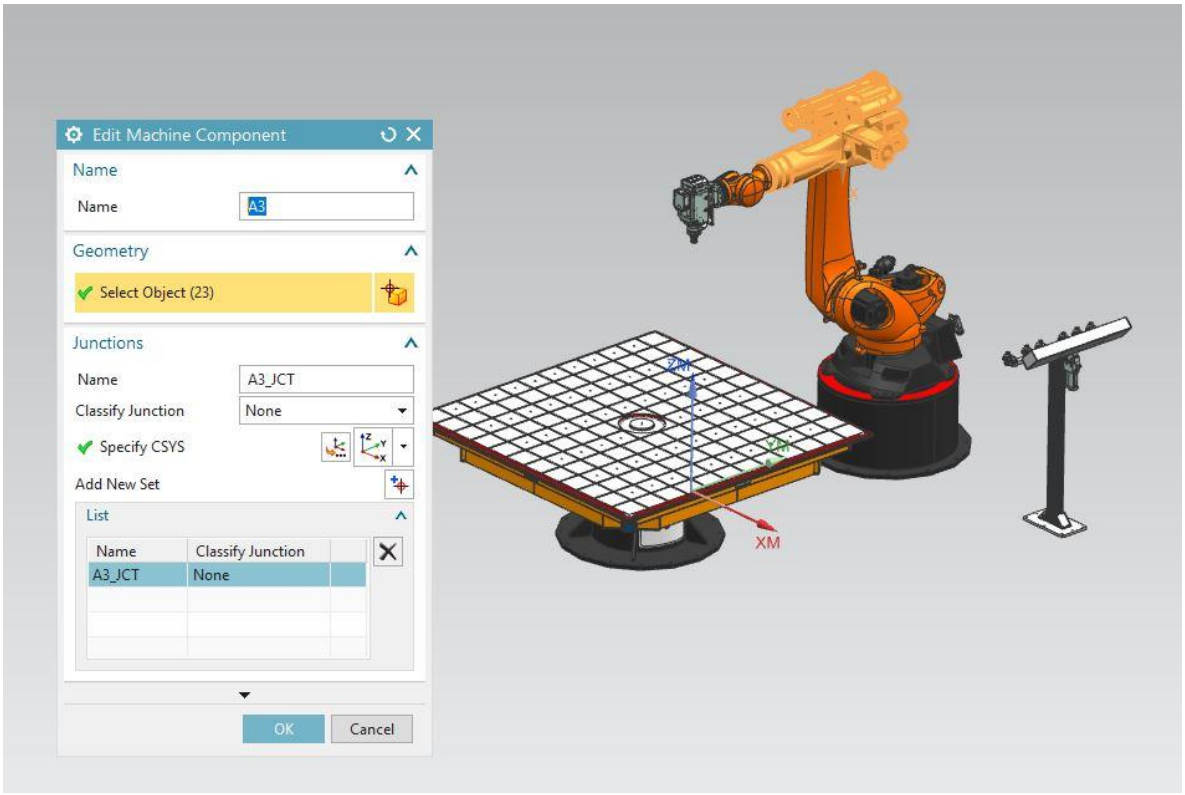

Figure 7-5: Third axis

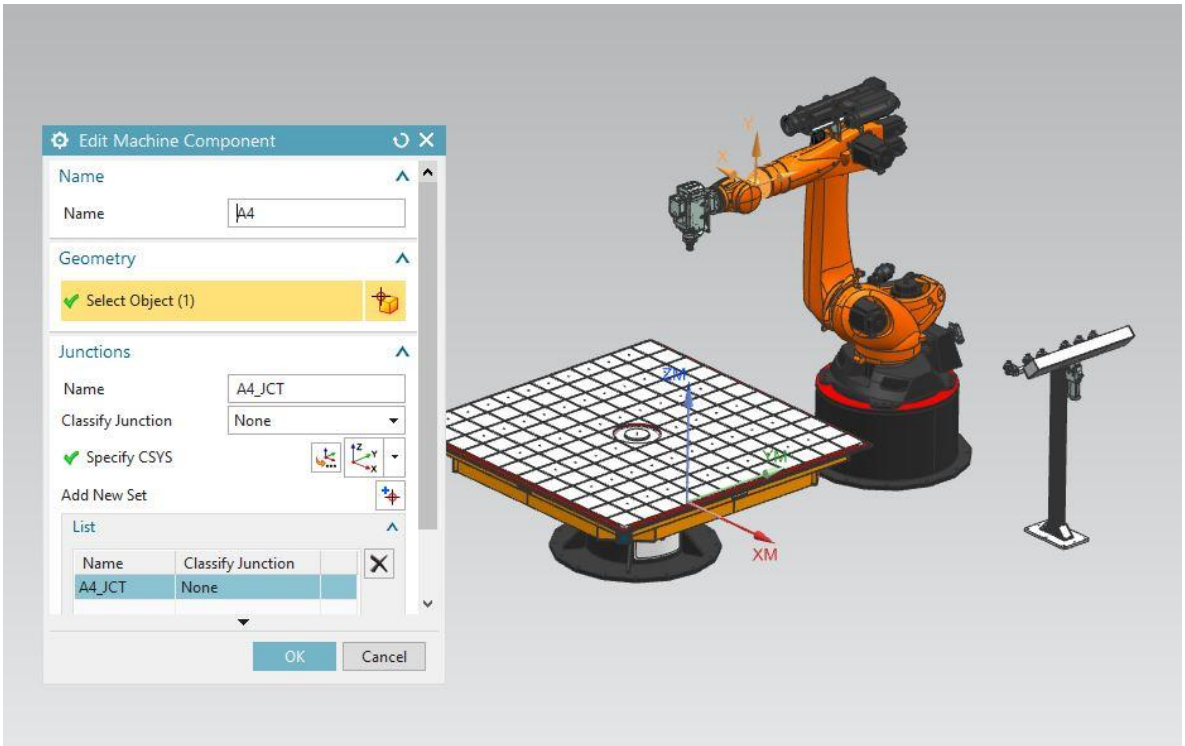

Figure 7-6: Fourth axis

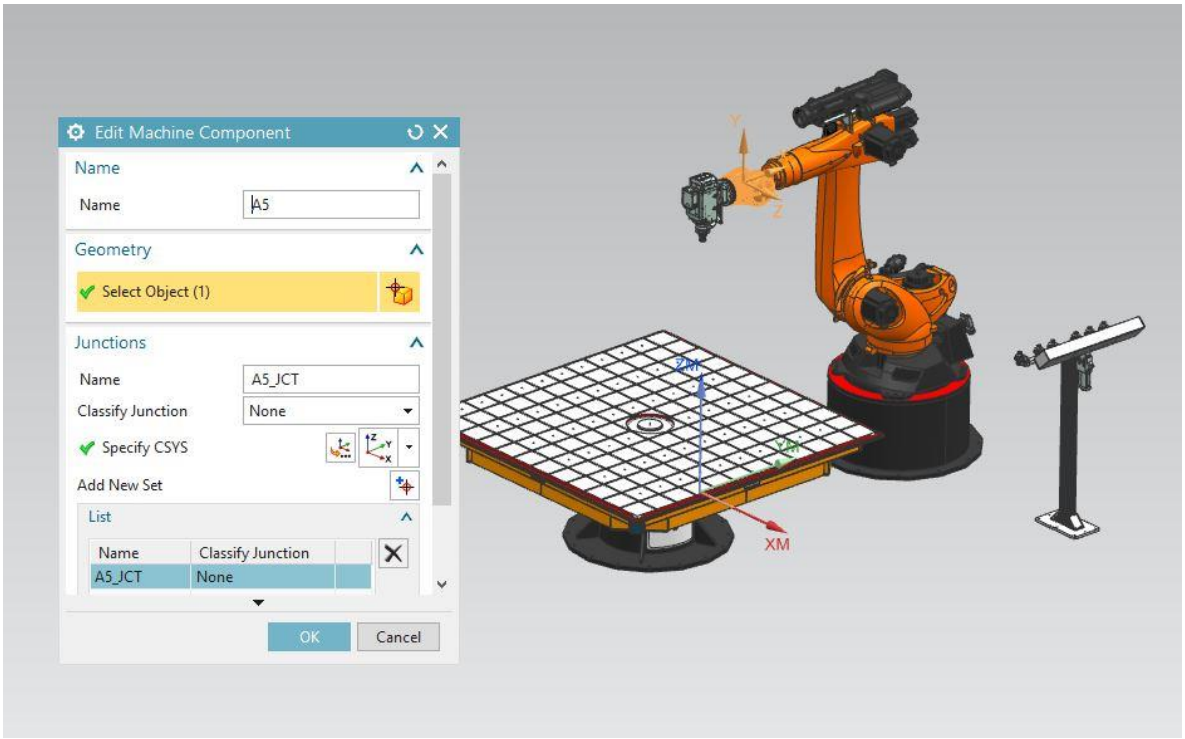

Figure 7-7: Fifth axis

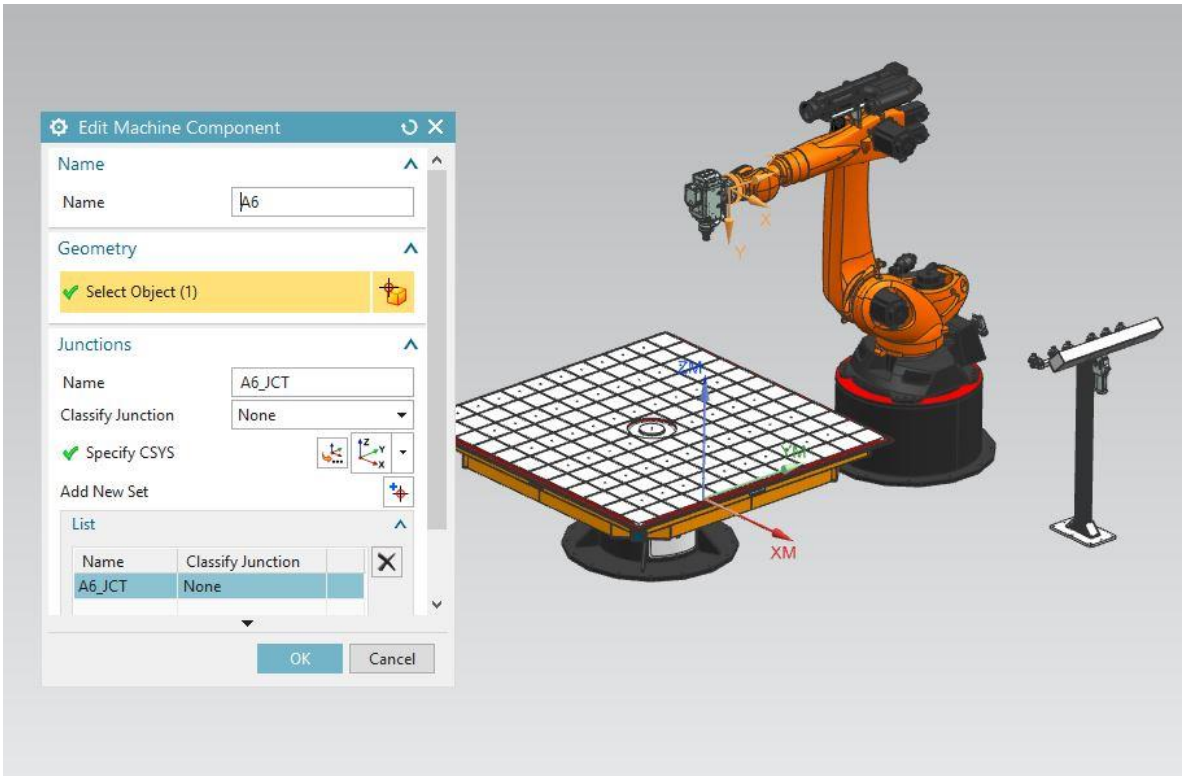

Figure 7-8: Sixth axis

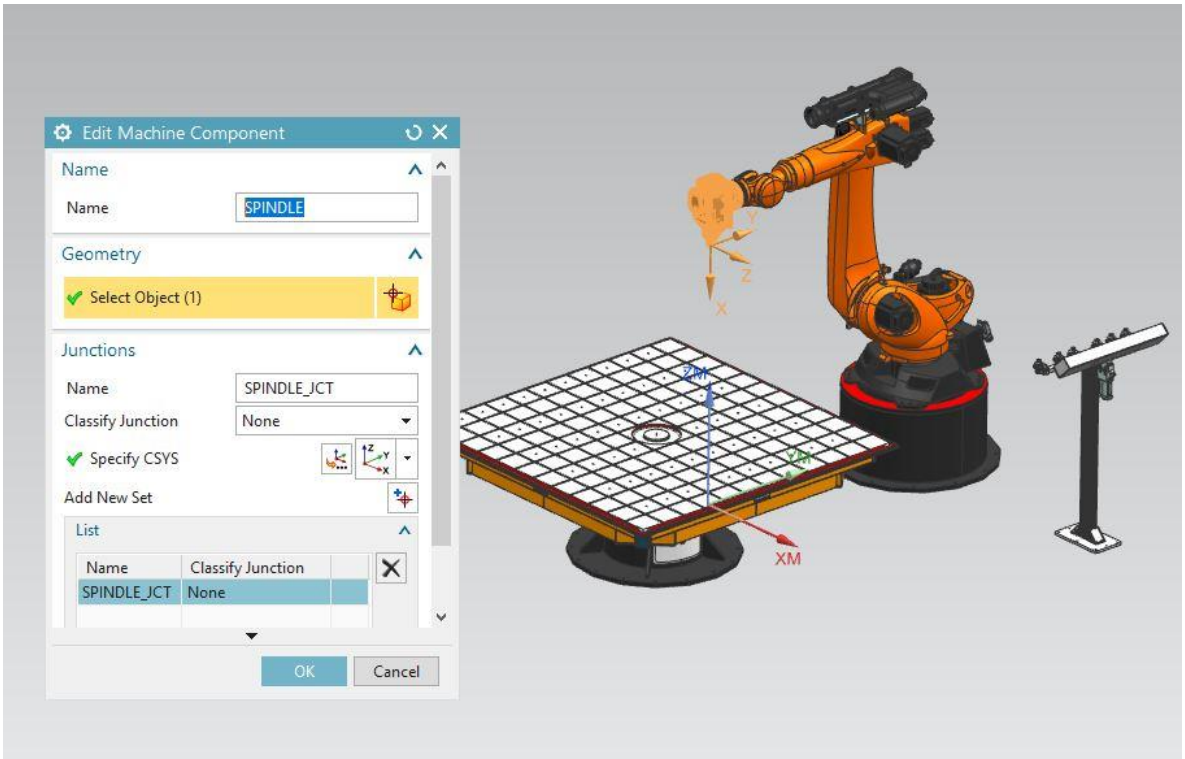

Figure 7-9: Spindle

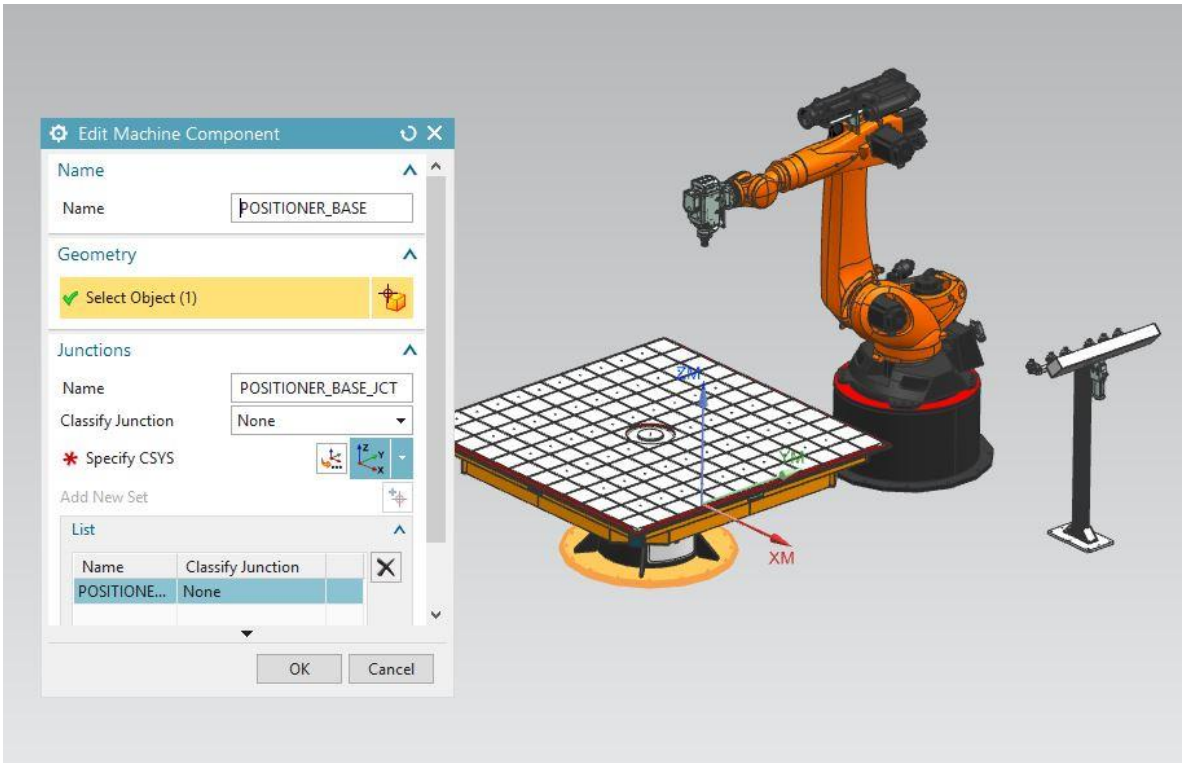

Figure 7-10: Positioner Base

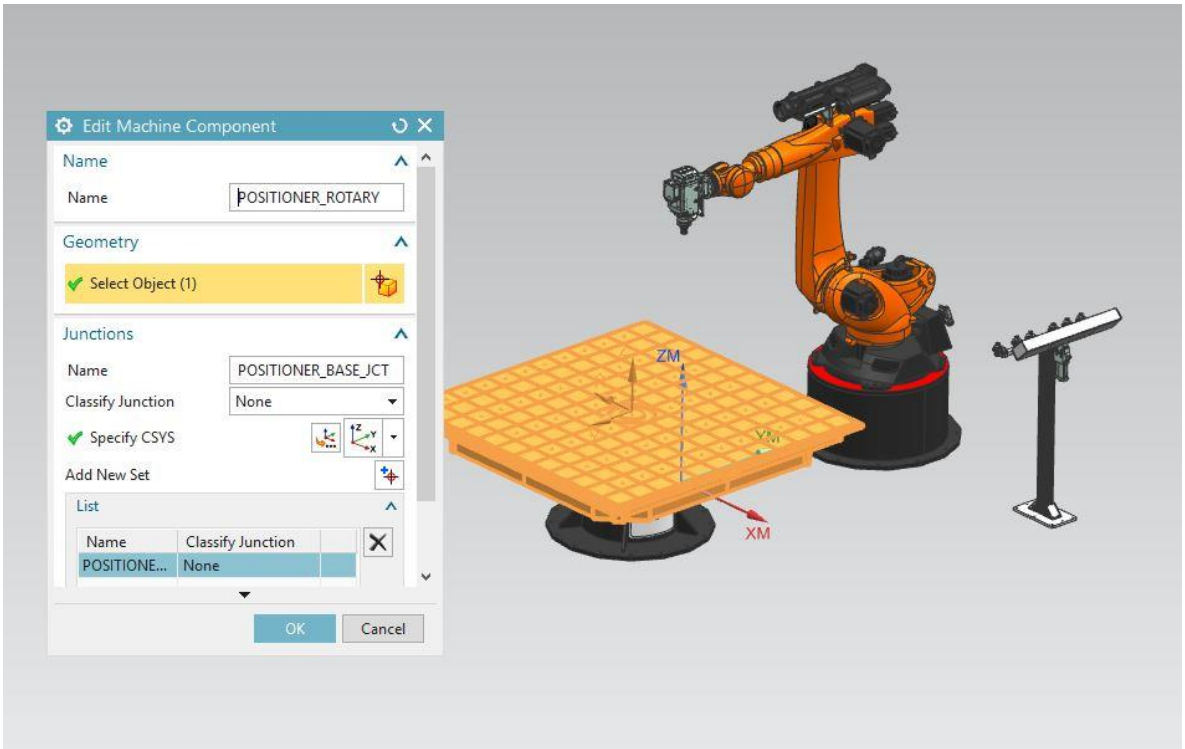

Figure 7-11: Positioner rotary table

All the joint properties are defined from the first joint until the positioner. Then finally the machine tool tree is constructed as below.

Name	Classification	Junctions	Axis Name	Initial Value	Axis Limits
KUKA_KR240					
MACHINE_BASE	_MACHINE_BASE	MACHINE_ZERO_JUNCTION*			
ROBOT_BASE		ROBOT_BASE_JCT			
A1		A1_JCT	A1	0	-185, 185
A2		A2_JCT	A2	-90	-140, -5
A3		A3_JCT	A3	90	-120, 155
A4		A4_JCT	A4	0	-350, 350
A5		A5_JCT	A5	0	-122.5, 122.5
A6		A6_JCT	A6	0	-350, 350
SPINDLE		SPINDLE_JCT			
POCKET	_DYNAMIC_HOLDER	POCKET_JCT			
POSITIONER_BASE					
POSITIONER_ROTARY		POSITIONER_BASE_JCT	POSITIONER	0	-180, 180
PART	_PART, _SETUP_ELEMENT	POSITIONER_ROTARY_JCT			

Figure 7-12: Machine tool tree

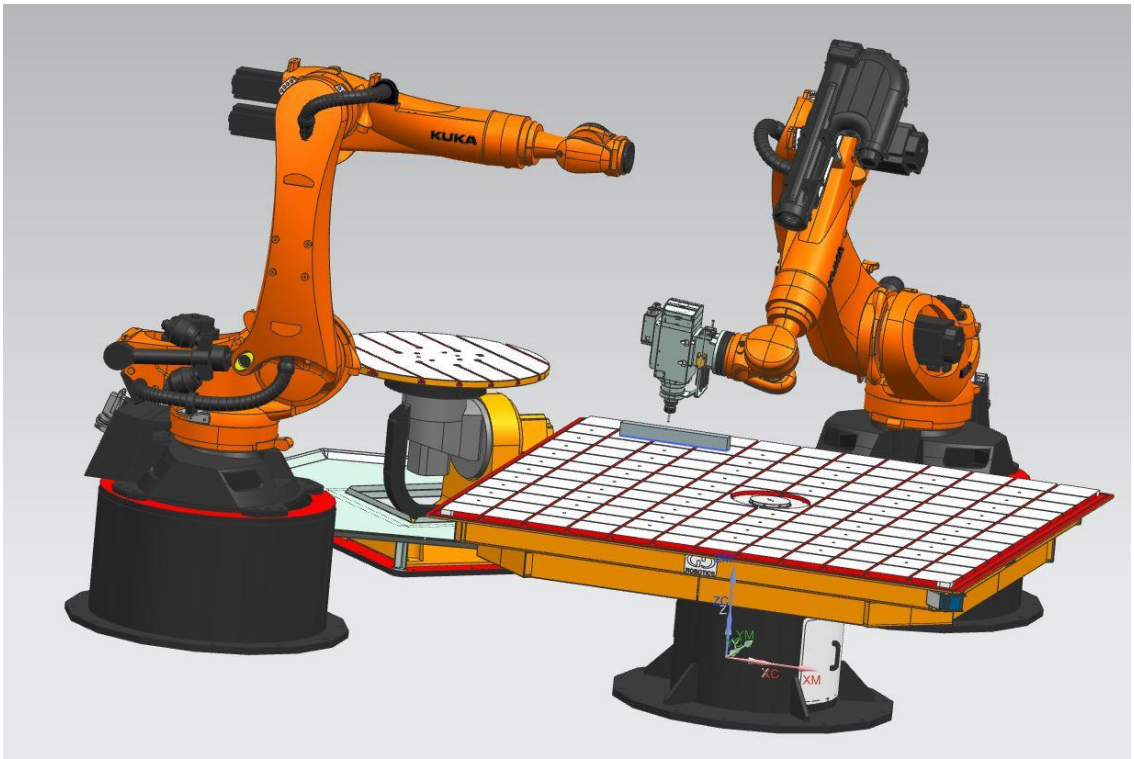

Figure 7-13: Robot cell during operation

In order to perform a cutting operation, the post-processor and the cad data of the robot should be placed in to following directory of the CAM software.

C:\Program Files\Siemens\NX 12.0\MACH\resource\library\machine\installed_machines

The implementation of the robot to CAM interface is a critical job due to safety regulations. So that the procedure abovementioned must not be used and performed without getting official help from the manufacturer side and CAM software.

8 BIBLIOGRAPHY

[1]Spong, Mark W., and Mathukumalli Vidyasagar. *Robot dynamics and control*. John Wiley & Sons, 2008.

[2]https://www.robotics.org/

[3]Pandremenos, J., Doukas, C., Stavropoulos, P., & Chryssolouris, G. (2011). Machining with robots: a critical review. *Proceedings of DET2011*, 1-9.

[4]https://www.kuka.com/

[5]Pandilov, Z., & Dukovski, V. (2014). Comparison of The Characteristics Between Serial And Parallel Robots. Acta Technica Corvininesis-Bulletin of Engineering, 7(1).

[6]Klimchik, A., Ambiehl, A., Garnier, S., Furet, B., & Pashkevich, A. (2016). Experimental study of robotic-based machining. IFAC-PapersOnLine, 49(12), 174-179.

[7]Klimchik, A., Ambiehl, A., Garnier, S., Furet, B., & Pashkevich, A. (2017). Efficiency evaluation of robots in machining applications using industrial performance measure. Robotics and Computer-Integrated Manufacturing, 48, 12-29.

[8]Hartenberg, R. S., & Denavit, J. (1955). A kinematic notation for lower pair mechanisms based on matrices. Journal of applied mechanics, 77(2), 215-221.

[9]Brandstötter, M., Angerer, A., & Hofbaur, M. (2014, May). An analytical solution of the inverse kinematics problem of industrial serial manipulators with an ortho-parallel basis and a spherical wrist. In Proceedings of the Austrian Robotics Workshop (pp. 7-11).

[10]Snyder, T. J., & Kazerooni, H. (1996, April). A novel material handling system. In Proceedings of IEEE International Conference on Robotics and Automation (Vol. 2, pp. 1147-1152). IEEE.

[11]Chen, H., Sheng, W., Xi, N., Song, M., & Chen, Y. (2002, May). Automated robot trajectory planning for spray painting of free-form surfaces in automotive manufacturing. In Proceedings 2002 IEEE International Conference on Robotics and Automation (Cat. No. 02CH37292) (Vol. 1, pp. 450-455). IEEE.

[12] Božek, P. (2013). Robot path optimization for spot welding applications in automotive industry. *Tehnicki Vjesnik–Technical Gazette*, *20*(5), 913-917.

[13]Rooks, B. (2003). Machine tending in the modern age. Industrial Robot: An International Journal, 30(4), 313-318.

[14]Matsuoka, S. I., Shimizu, K., Yamazaki, N., & Oki, Y. (1999). High-speed end milling of an articulated robot and its characteristics. Journal of materials processing technology, 95(1-3), 83-89.

[15]Iglesias, I., Sebastián, M. A., & Ares, J. E. (2015). Overview of the state of robotic machining: Current situation and future potential. Procedia engineering, 132, 911-917.

[16]Budak, E., Ozturk, E., & Tunc, L. T. (2009). Modeling and simulation of 5-axis milling processes. CIRP annals, 58(1), 347-350.

[17]Jun, C. S., Cha, K., & Lee, Y. S. (2003). Optimizing tool orientations for 5-axis machining by configuration-space search method. Computer-Aided Design, 35(6), 549-566.

[18]Ozturk, E., & Budak, E. (2007). Modeling of 5-axis milling processes. Machining Science and Technology, 11(3), 287-311.

[19]Tunc, L. T., Budak, E., Bilgen, S., & Zatarain, M. (2016). Process simulation integrated tool axis selection for 5-axis tool path generation. CIRP Annals, 65(1), 381-384.

[20]Makhanov, S. S., & Munlin, M. (2007). Optimal sequencing of rotation angles for five-axis machining. The International Journal of Advanced Manufacturing Technology, 35(1-2), 41-54.

[21]Munlin, M., Makhanov, S. S., & Bohez, E. L. (2004). Optimization of rotations of a five-axis milling machine near stationary points. Computer-Aided Design, 36(12), 1117-1128.

[22]Abele, E., Weigold, M., & Rothenbücher, S. (2007). Modeling and identification of an industrial robot for machining applications. CIRP annals, 56(1), 387-390.

[23]Dumas, C., Caro, S., Garnier, S., & Furet, B. (2011). Joint stiffness identification of six-revolute industrial serial robots. Robotics and Computer-Integrated Manufacturing, 27(4), 881-888.

[24]Abele, E., Rothenbücher, S., & Weigold, M. (2008). Cartesian compliance model for industrial robots using virtual joints. Production Engineering, 2(3), 339.

[25]Klimchik, A., Ambiehl, A., Garnier, S., Furet, B., & Pashkevich, A. (2017). Efficiency evaluation of robots in machining applications using industrial performance measure. Robotics and Computer-Integrated Manufacturing, 48, 12-29.

[26]Zaeh, M. F., & Roesch, O. (2014). Improvement of the machining accuracy of milling robots. Production Engineering, 8(6), 737-744.

[27]Schneider, U., Drust, M., Ansaloni, M., Lehmann, C., Pellicciari, M., Leali, F. & Verl, A. (2016). Improving robotic machining accuracy through experimental error investigation and modular compensation. The International Journal of Advanced Manufacturing Technology, 85(1-4), 3-15.

[28]Pan, Z., Zhang, H., Zhu, Z., & Wang, J. (2006). Chatter analysis of robotic machining process. Journal of materials processing technology, 173(3), 301-309.

[29]Zaghbani, I., Songmene, V., & Bonev, I. (2013). An experimental study on the vibration response of a robotic machining system. Proceedings of the Institution of Mechanical Engineers, Part B: Journal of Engineering Manufacture, 227(6), 866-880.

[30]Tunc, L. T., & Shaw, J. (2016). Experimental study on investigation of dynamics of hexapod robot for mobile machining. The International Journal of Advanced Manufacturing Technology, 84(5-8), 817-830.

[31]Tunc, L. T., & Stoddart, D. (2017). Tool path pattern and feed direction selection in robotic milling for increased chatter-free material removal rate. The International Journal of Advanced Manufacturing Technology, 89(9-12), 2907-2918.

[32]Pessoles, X., Landon, Y., Segonds, S., & Rubio, W. (2013). Optimisation of workpiece setup for continuous five-axis milling: application to a five-axis BC type machining centre. The International Journal of Advanced Manufacturing Technology, 65(1-4), 67-79.

[33]Yang, J., Aslan, D., & Altintas, Y. (2018). Identification of workpiece location on rotary tables to minimize tracking errors in five-axis machining. International Journal of Machine Tools and Manufacture, 125, 89-98.

[34]Anotaipaiboon, W., Makhanov, S. S., & Bohez, E. L. (2006). Optimal setup for five-axis machining. International Journal of Machine Tools and Manufacture, 46(9), 964-977.

[35]Lin, Z., Fu, J., Shen, H., & Gan, W. (2014). On the workpiece setup optimization for five-axis machining with RTCP function. The International Journal of Advanced Manufacturing Technology, 74(1-4), 187-197.

[36]Caro, S., Dumas, C., Garnier, S., & Furet, B. (2013). Workpiece Placement Optimization in Robotic-based Manufacturing. IFAC Proceedings Volumes, 46(9), 819-824.

[37]Lopes, A. M., & Pires, E. S. (2011). Optimization of the workpiece location in a machining robotic cell. International Journal of Advanced Robotic Systems, 8(6), 73.

[38]Lin, Y., Zhao, H., & Ding, H. (2017). Posture optimization methodology of 6R industrial robots for machining using performance evaluation indexes. Robotics and Computer-Integrated Manufacturing, 48, 59-72.

[39]Vosniakos, G. C., & Matsas, E. (2010). Improving feasibility of robotic milling through robot placement optimisation. Robotics and Computer-Integrated Manufacturing, 26(5), 517-525.

[40]Varshalovich, D. A., Moskalev, A., & Khersonskii, V. (1988). Description of rotation in terms of the euler angles. Quantum Theory of Angular Momentum, World Scientific.

[41]Ottaviano, E., Husty, M., & Ceccarelli, M. (2006, May). A study on workspace topologies of 3r industrial-type manipulators. In 2006 IEEE International Conference on Automation, Quality and Testing, Robotics (Vol. 2, pp. 237-242). IEEE.

[42]Peiper, D. L. (1968). The kinematics of manipulators under computer control (No. CS-116). STANFORD UNIV CA DEPT OF COMPUTER SCIENCE.

[43]Craig, J. J. (2009). Introduction to robotics: mechanics and control, 3/E. Pearson Education India.

[44]https://www.mathworks.com/products/matlab.html

[45]https://www.plm.automation.siemens.com/global/en/products/nx/

[46] Tunç, T. L. (2006). Geometrical Analysis and Optimization of 5-Axis Milling Processes (Doctoral dissertation).

[47]Tunc, L. T. (2016). Rapid extraction of machined surface data through inverse geometrical solution of tool path information. The International Journal of Advanced Manufacturing Technology, 87(1-4), 353-362.

[48]https://www.mathworks.com/help/matlab/ref/graph.shortestpath.html